Marine and Coastal

National Environmental Science Program

FINAL REPORT

Project 3.13

September 2025

Eastern grey nurse shark, *Carcharias taurus*, population abundance and trend

Russell W Bradford[1a], David Harasti[2a], Emma L Westlake[1b], Robin Thomson[1a], Pierre Feutry[1a], Shane Baylis[1a], Ben Mayne[1c], Chloe Anderson[1b], Rich Hillary[1a], Rasanthi Gunasekera[1a], Paul Butcher[2b], Brett Louden[2a], Christopher Gallen[2a], Toby A Patterson[1a]

CSIRO

NSW GOVERNMENT

Milestone number 6: Final Report

Research Plan 2023: Project 3.13

Please address inquiries to: Russell Bradford: russ.bradford@csiro.au

Preferred citation

Bradford, R.W., Harasti, D., Westlake, E. L., Thomson, R., Feutry, Baylis, S., P., Mayne, B., Anderson, C., Hillary, R., Gunasekera, R., Butcher, P., Louden, B., Gallen, C., Patterson, T.A. (2025). NESP2 MaC Hub Project 3.13: Eastern grey nurse shark, *Carcharias taurus*, population abundance and trend. Report to the National Environmental Science Program. CSIRO Environment, Hobart, Tasmania.

Copyright ©

[1a] CSIRO Environment. GPO Box 1538, Hobart, TAS, 7001

[1b] CSIRO Environment. Bayview Avenue/Research Way, Clayton, VIC, 3168

[1c] Flinders University, College of Medicine and Public Health. Sturt Road, Bedford Park, SA 5042

[2a] New South Wales Department Primary Industries and Regional Development, Fisheries Research. Port Stephens Fisheries Institute, Taylors Beach, NSW 2316

[2b] New South Wales Department Primary Industries and Regional Development, Fisheries. PO Box 4321, National Marine Science Centre, Coffs Harbour, NSW 2450

This report is reproduced and made available under the following licence from the copyright owners: Creative Commons Attribution 4.0 Australia Licence.

For licence conditions, see https://creativecommons.org/licenses/by/4.0/

Acknowledgement

This work was undertaken for the Marine and Coastal Hub, a collaborative partnership supported through funding from the Australian Government's National Environmental Science Program (NESP).

Animal Ethics Authority

NSW Fisheries Research Animal Ethics Committee. FR ARA 447: Grey Nurse Shark (*Carcharias taurus*) genetics Project. 17 November 2022–16 November 2025.

NESP Marine and Coastal Hub partners

The Australian Institute of Marine Science, Bioplatforms Australia, Bureau of Meteorology, Charles Darwin University, Central Queensland University, CSIRO, Deakin University, Edith Cowan University, Flinders University, Geoscience Australia, Griffith University, Integrated Marine Observing System, James Cook University, Macquarie University, Murdoch University, Museums Victoria, NSW Department of Planning and Environment (Environment, Energy and Science Group), NSW Department of Primary Industries, South Australian Research and Development Institute, The University of Adelaide, University of Melbourne, The University of Queensland, University of New South Wales, University of Tasmania, University of Technology Sydney, The University of Sydney, University of Western Australia, The University of Wollongong

Disclaimer

The NESP Marine and Coastal Hub advises that this publication comprises general statements based on scientific research. The reader is advised and needs to be aware that such information may be incomplete or unable to be used in any specific situation. No reliance or actions must therefore be made on that information without seeking prior expert professional, scientific and technical advice. To the extent permitted by law, the NESP Marine and Coastal Hub (including its host organisations, employees, partners and consultants) excludes all liability to any person for any consequences, including but not limited to all losses, damages, costs, expenses and any other compensation, arising directly or indirectly from using this publication (in part or in whole) and any information or material contained in it.

Cover images: David Harasti (NSW DPIRD)

This report is available on the NESP Marine and Coastal Hub website:
www.nespmarinecoastal.edu.au

Acknowledgments

This project has relied on collaborations across Australia. We would like to thank Mike Travers (WA DPIRD) and his team for providing grey nurse shark tissue samples from Western Australian. Samples from the Northern Territory were provided by Michael Usher (NT DITT, Fisheries) and Suzanne Horner (MAGNT). Floriaan Devloo-Delva (CSIRO) applied his expertise to extracting DNA from the NT sample that had been preserved in formalin as well as genetically confirming both NT samples were *Carcharias taurus*. Dr Nicholas Otway (NSW DPIRD) is thanked for providing access to the raw vertebral ageing data used here to develop a growth curve.

Contents

List of figures

List of tables

Acronyms

ATF	Animal Tracking Facility
CJS	Cormack-Jolly-Seber
CKMR	Close-Kin Mark-Recapture
CpG	cytosine-phosphate-guanine
CSIRO	Commonwealth Scientific and Industrial Organisation
DArT	Diversity Arrays Technology
DOSV	Diver Operated Stereo Video
EPBC Act	*Environment Protection and Biodiversity Conservation (EPBC) Act* 1999
FSP	Full Sibling Pair
GGP	Grandparent Grandchild Pair
GNS	Grey Nurse Shark
HCP	Half Cousin Pair
HSP	Half Sibling Pair
HTP	Half Thiatic Pair
IMOS	Integrated Marine Observing System
MAGNT	Museum and Art Gallery Northern Territory
MCMC	Markov chain Monte Carlo
MH	Metropolis-Hastings
NSW DPIRD	New South Wales Department of Primary Industries and Regional Development
NT DITT	Northern Territory Department of Industry, Tourism and Trade
PLOD	Pseudo Log Odds
POP	Parent-Offspring Pair
SMART	Shark Management Alert in Real Time
UP	Unrelated Pair
VBGF	Von Bertalanffy Growth Function

Executive summary

In Australia, there are two separate populations of grey nurse shark (GNS): a Western Australian population listed as Vulnerable, and an eastern Australian population listed as Critically Endangered under the EPBC Act (1999). This report provides an estimate of abundance and trend in abundance for the adult component of the eastern Australian population using the Close-Kin Mark-Recapture (CKMR) method.

CKMR is a powerful tool that relies on genetically identifying related individuals. The basic premise being that the degree of relatedness within the sampled population will provide an estimate of adult abundance. Twenty-one Parent-Offspring (POP) pairs, six Full Sibling (FSP) pairs, and 148 Half Sibling (HSP) pairs were identified in the dataset. All POPs and 146 HSPs passed QC and were used in deriving an estimate of abundance. FSPs are not used in the CKMR model.

Adult GNS abundance in 2023 is estimated to be 1,423 (95% CI: 921 to 1925 adults; CV[1] = 0.18) adults. The model further estimates the annual rate of increase to be 5% (95% CI: 2.3 – 7.1%). We would expect this to be close to the maximum rate of increase for this species. The current estimate uses a refined genetic method and a revised dataset from newly collected samples, resulting in fewer data being discarded due to the use of an Australian-specific growth curve to identify related individuals. This has resulted in an update of the previously reported abundance estimate (N_{2017}) to 1,096 adults (CV = 0.15).

The NSW DPIRD provided data from necropsied GNS that have allowed for the derivation of a growth curve specific to the eastern Australian GNS population. The Australian growth curve has resulted in a CKMR model that performs better than when using a growth curve from USA GNS.

Acoustic tagging projects undertaken in NSW have provided an opportunity to investigate juvenile survival rates. Survival is expected to be high for GNS based on their low reproductive output strategy. Initial results indicate juvenile survival for ages 0 to 4 to be approx. 85% per annum, with survival of older ages increasing to at least 90% per annum. This result, however, should be taken with caution due to the small sample size and possible male bias. However, the results indicate that there is information on survival from telemetry data from internally implanted long-life acoustic tags, but any further tagging should focus on females and the youngest available animals.

The work undertaken by NSW DPIRD to develop an age-at-length key has allowed us to investigate a genetic method to estimate age, called epigenetic ageing. Unfortunately, the

[1] The CV, or coefficient of variation, is the ratio of the standard deviation to the mean. The higher the coefficient of variation, the greater the level of dispersion around the mean.

number of samples was too small to develop an epigenetic model of age for GNS. Further research is required to tailor epigenetic methodology for shark and ray species.

A single DNA sample provided by Northern Territory Fisheries was compared to DNA from both the eastern and western GNS populations. The NT sample genetically aligns more closely with known western GNS samples than it does to the known eastern GNS samples.

1. Introduction

The grey nurse shark (*Carcharias taurus*; GNS) is a large migratory coastal shark species belonging to the family Odontaspididae. It has a global distribution in subtropical and warm temperate waters (Compagno 2001) and is known to aggregate in deep sandy gutters. Due to its susceptibility to fishing pressure, historical overfishing, and low reproductive rates, the International Union for Conservation of Nature (IUCN) Red List has assessed the GNS as Critically Endangered (IUCN 2023).

In Australia, GNS have been recorded in all coastal waters, except those of Tasmania (Last and Stevens 2009), with sightings most frequent in Queensland, New South Wales, and Western Australia. Genetic evidence indicates that within Australia, GNS can be divided into two distinct populations: GNS from Queensland and NSW comprising the eastern population and those in Western Australia comprising the western population (Stow et al. 2006), with negligible or no migration between these populations (Ahonen & Stow 2009).

Low levels of genetic diversity increase the risk of extinction in the eastern Australia GNS population, with the eastern GNS listed as Critically Endangered under the *Environment Protection and Biodiversity Conservation (EPBC) Act* 1999. Accordingly, a strategy to promote recovery of the GNS population in eastern Australia was implemented in 2002 with the development of the first recovery plan (EA 2002). Since then, the recovery plan has been reviewed twice (DEWHA 2009; DoE 2014), detailing several advances made in the conservation of the species. However, the 2014 recovery plan (DoE 2014) states two key areas that require ongoing research:

- *improving the population status leading to the removal of the grey nurse shark from the threatened species list of the EPBC Act; and*
- *ensuring that anthropogenic activities do not hinder the recovery of the grey nurse shark in the near future, or impact on the long-term conservation status of the species.*

Population abundance is the primary metric used to inform recovery. In 2018, the CSIRO and New South Wales Department of Primary Industries (NSW DPI), with partners in Queensland and Victoria, provided the first robust estimate of adult abundance for the eastern GNS population (Bradford et al. 2018). This estimate indicated that the adult population was approx. 2000 (950-3100 individuals) and that the trend in abundance was highly likely to be increasing at a rate of approximately 3-4% per annum. Bradford et al. (2018) concluded that recovery actions were effective, however, easing of protective measures was not recommended, in part due to the uncertainty in estimating abundance with poor growth data available at that time.

Following the publication of the GNS abundance estimate in 2018 (Bradford et al. 2018), NSW DPIRD have progressed vertebral ageing of GNS using archived samples. Although that work is yet to be published (N. Otway, pers comm.), this project has been granted access to some of these data to use in developing a growth curve for Australian GNS. Additionally, epigenetic ageing is an emerging technique for ageing marine animals (Mayne et al. 2021). The appeal of this method lies in the potential to estimate age from genetic data alone once calibrated to existing age estimates. While it is yet to be investigated in detail for elasmobranchs, tissue samples from vertebral-aged animals provide an opportunity to investigate this technique in elasmobranchs.

This study proposes to update the eastern Australian GNS abundance estimate by incorporating recent advances such as epigenetic ageing, and to employ improved sampling protocols to obtain greater precision in length measurements. This will reduce bias in the

abundance estimate, while the combination of additional new samples with those previously collected, should reduce the uncertainty around the trend in abundance.

Overall, the key components of the project are:

- To derive a contemporary Close-Kin Mark-Recapture abundance estimate for the eastern Australian GNS population.
- To use a new dataset of tissue samples collected by SCUBA with divers using stereo video analysis to obtain accurate length measurements of sampled sharks (reducing uncertainty in age assignment).
- To investigate epigenetic ageing of juvenile GNS using tissue samples with vertebral age (collected by a recent project by NSW DPIRD).
- To use growth curves derived from Australian GNS samples involved in an ageing project undertaken by NSW DPIRD in subsequent CKMR modelling.

2. Abundance estimation for eastern Australian *Carcharias taurus*

2.1 Background

Carcharias taurus (grey nurse shark, GNS) is distributed throughout warm-temperate and tropical coastal waters of the Mediterranean Sea, Atlantic and Indo-West Pacific Oceans (Compagno 2001). In Australia, GNS have been observed in all Australian coastal waters, except Tasmania (Last and Stevens, 2009), however, are rarely observed in South Australia, Victoria, and the Northern Territory. Although GNS inhabit waters to at least 190 m depth, they are most commonly observed in shallow waters where they aggregate in gullies and caves (Pollard et al., 1996, Otway & Burke 2004).

The reproductive strategy of GNS is well described (see Pollard et al., 1996, Gilmore et al., 1983, Compagno 2001, Otway & Burke 2004). Grey nurse shark has an ovoviviparous reproductive strategy whereby embryos feed on ova after the yolk sac has been consumed, followed by intra-uterine cannibalism, resulting in a maximum of two pups per litter (Pollard et al. 1996, Compagno 2001, Bansemer & Bennett 2009). Reproduction has a biennial cycle (Bansemer & Bennett 2009) that includes a gestation period of 9-12 months followed by a 12-month rest cycle (Gordon 1993, Compagno 2001). Females mature at approximately 220 cm (total length, TL) and males slightly smaller at approximately 190 cm TL (Gilmore et al., 1983, Lucifora et al., 2002), with age at sexual maturity of 9-10 years for females, and 6-7 years for males (Goldman et al., 2006).

Prior to the 1960s, GNS were widespread and abundant along the eastern Australian seaboard (Cropp 1964). However, a range of anthropogenic pressures from the 1960s, particularly spearfishing led to a decline in observed numbers, until full protection was implemented in 2001. Pepperell (1992) reported a decline in catch rates in gamefish records from 11% in the 1960s to 7% in the 1970s. Further evidence was observed in the catch records of the New South Wales Shark Meshing Program, where catch rates showed a consistent downward trend from the 1950s to 2010, with an estimated reduction in catch rates of 97% over that period (Reid et al., 2011).

The combination of a distribution that allowed for easy and widespread exploitation, low rate of intrinsic recovery due to their reproductive strategy and observed decline in abundance led to the implementation of various forms of protection from 1979 (Pepperell 1992), with full protection afforded in 1997 under the *Endangered Species Protection Act* (1992); then under the *Environmental Protection and Biodiversity Conservation Act* (EPBC 1999). The current recovery plan for GNS (DoE 2014) lists ten objectives, which includes 35 actions. This study provides input into three of the recovery plan's objectives and at least six actions (Table 1).

Table 1: Recovery Plan Objectives (DoE 2014).

Objective	Action	Priority Level	Description
Objective 1: Develop and apply quantitative monitoring of the population status (distribution and abundance) and potential recovery of the grey nurse shark in Australian waters.	1.1	1	Monitor and re-survey GNS populations to assess population trends and dynamics, including estimates of population growth and mortality.
Objective 1:	1.3	2	Evaluate the use of and develop new population models, using reliable data sets as they are collected, to reassess changes in extinction risks.
Objective 9: Continue to develop and implement research programs to support the conservation of the grey nurse shark.	9.1	2	Collect, analyse and disseminate age, growth, reproduction, survival, mortality and diet information to further improve understanding of the population dynamics and habitat requirements of the GNS.
Objective 9:	9.2	2	Continue to collect and analyse biological material for toxicology research and genetic analysis (for example to determine the stock structure, inbreeding depression, population boundaries and abundance), improve coordination of reporting and sampling programs and coordinate the collation of results and the storage of collected genetic, biological and toxicological material (Link to Action 7.1).
Objective 10: Promote community education and awareness in relation to grey nurse shark conservation and management.	10.1	1	Update DoE's GNS recovery plan web page to reflect the most current information on the grey nurse shark. Ensure the web page is presented in a form that is easily understood by the public and is linked to the relevant website(s) of other jurisdictions with an interest in conservation of grey nurse sharks.
Objective 10:	10.4	2	Encourage community involvement in collaborative research, monitoring and education.

Assessing the efficacy of recovery actions requires knowledge of contemporary abundance and historical trends in abundance informing Objectives 1 and 9 of the recovery plan. There have been several studies aimed at estimating GNS abundance with the first being published

in 2004 (Otway and Burke, 2004) and the latest by Bradford et al. in 2018 (Table 2). These estimates of abundance have incorporated several different approaches (physical mark-recapture, photo-ID, genetic mark-recapture), each with its own set of assumptions and limitations (e.g., low sample size, limited re-sighting/tagging, limited spatial distribution in sampling, poor age estimation).

Table 2: Abundance estimates for eastern Australian grey nurse shark reported in the scientific literature. “est” is the abundance estimate provided in the respective publication.

Study	**Type**	**# sharks**	**Life stage**	**Lower**	**Upper**	**Abundance (year)**
Otway & Burke 2004 (Petersen method)	Mark-Recapture	24 (mark) 16 (recapture)	All	410	461	*148-766 (2003)
Otway & Burke 2004 (Petersen method)	Mark-Recapture	22 (mark) 16 (recapture)	Adult	161	194	*58-321 (2003)
Cardno 2010	Photo-ID M-R	590 (photo) 66 (Re-sightings)	All	1104 **885	1601 **1376	1315 (est) **1131 (est) (2009)
Cardno 2010 (adjusting for ‘unmarkable’ portion)	Photo-ID M-R	590 (photo) 66 (Re-sightings)	All	1146 **919	1662 **1429	1365 (est) **1174 (est) (2009)
Cardno 2010 (adjusting for site fidelity)	Photo-ID M-R	590 (photo) 66 (Re-sightings)	All	1465 **1216	3249 **2883	2142 (est) **2049 (est) (2009)
Bansemer 2009 (Jolly-Seber open model design)	Photo-ID M-R		All	590 (males) 901 (females)	922 (males) 1469 (females)	756 (males) 1185 (females) (2008)
Ahonen & Stow 2009	Genetic (microsatellites)	87 (total) 63 (EA GNS) 24 (WA GNS)	ŧ Ne	~68	~474	1000-1500 (total abundance) (2009)
Bradford et al. 2018 ***(scenario 1)	Close-Kin Mark-Recapture (genetic)	378 (from 489 following strict QC)	Adult	1257	3078	2167 (est) (2017)
Bradford et al. 2018 ****(scenario 2)	Close-Kin Mark-Recapture (genetic)	378 (from 489 following strict QC)	Adult	956	2417	1686 (est) (2017)

*Note several methods of calculation are reported in Otway & Burke 2004 – here the minimum and maximum across all methods has been reported (see Tabel 4.1 Otway & Burke 2004 for more detail).

**Bailey’s Binomial Modification applied for better comparison to Otway & Burke 2004.

***Scenario 1: Maturity set to 10 years (female) and 7 years (male).

****Scenario 2: Maturity set to 14 years (females) and 11 years (males).

ŧ Effective population size.

This project uses Close-Kin Mark-Recapture (CKMR) to derive an estimate of abundance and trend. CKMR uses a powerful combination of conventional mark-recapture theory and modern genetics (Bravington et al., 2016a). Specifically, rather than using physical marks or tags, "recaptures" are of an animal's close relatives, rather than of the actual animal itself. This allows for the use of samples from dead animals, and circumvents some problems of standard mark-recapture, such as local site fidelity. DNA profiles of individuals, derived from tissue samples, are compared across all individuals in the collection using the most up-to-date genotyping techniques to find related individuals (Parent-Offspring Pairs [POP], Full Sibling Pairs [FSP], Half Sibling Pairs [HSP], as well as Grandparent-Grandchild Pairs [GGPs] which are not distinguished genetically from HSPs). Given adequate sampling, the proportion of kin-pairs found and their spread in space and time can be used in a mathematically sound and transparent mark-recapture framework to estimate adult abundance, movement patterns, and trend (Bravington et al., 2016b).

Close-Kin Mark-Recapture was first successfully applied to southern bluefin tuna (*Thunnus maccoyii*; Bravington et al., 2016a). It has subsequently been used to derive estimates of abundance for both the eastern Australian and southern-western Australian populations of white shark (*Carcharodon carcharias*; Bruce et al., 2018; Hillary et al., 2018), school shark (Thomson et al., 2020), speartooth shark (Patterson et al., 2022), sawfish (NESP 3.11 https://www.nespmarinecoastal.edu.au/project/3-11/ & NESP 4.18: Indigenous Ranger-led monitoring of threatened sawfish in the southern Gulf of Carpentaria), and GNS (Bradford et al., 2018).

This study will provide an update to the eastern Australian GNS abundance estimate reported in Bradford et al. (2018). Using growth data from Australian GNS will also improve the estimate of trend in the GNS population.

2.2 Methods

2.2.1 Tissue collection

A largely new collection of tissue samples were obtained from three primary sources: a) targeted SCUBA diving surveys (live animals); b) NSW SMART drumline bycatch (live animals); and c) tissue samples from necropsied animals that were also used for a study on vertebral ageing. Some tissue samples used for the 2018 CKMR abundance estimate (Bradford et al., 2018) where length was accurately measured were included in the new analysis.

Tissue samples from live animals were collected by SCUBA divers trained in safe biopsy techniques using a hollow stainless-steel biopsy tip (6.250 mm external/5.450 mm internal diameter) attached to a hand spear, with a purpose-built quick release adaptor to allow divers to easily remove and replace biopsy tips while underwater. A diver would approach a shark underwater and when within close range, would obtain a small tissue sample using the biopsy tip. The biopsy tip containing the tissue sample was removed and placed in a numbered box and a new biopsy tip locked into the adaptor ready to sample another shark. At the same time as the tissue sample was being taken, a second diver using a diver operated stereo video (DOSV) would record imagery to provide for length estimation using Eventmeasure 6.44 software (www.seagis.com.au).

Divers would continue sampling sharks until all biopsy tips had been used, or of the majority of sharks present at the site had been sampled. For this project, sharks were only sampled on the lefthand side of the shark directly below the first dorsal fin. This was adhered to as it minimised the chance of the same shark being sampled twice. Identifying previously sampled

sharks was relatively easy, as the biopsy left a small wound in the same location which was recognisable for a period of several weeks (D. Harasti, pers. comm.). At the end of each dive, the tissue sample in each biopsy tip was removed and immediately placed into a DNA stabilising solution and given a unique identifying code for the site where the sample was collected. Analysis of the stereo-video footage collected allowed an accurate length measurement to be obtained, as well as the sex of the shark (based on the presence/absence of claspers). On the occasions where a stereo-length estimate was not obtained by the camera, due to camera failure or the shark not being recorded at an appropriate angle, a length estimate was provided by the divers. Accurate sex identification was not always possible but was later corrected using a DNA sex marker specific to male GNS (Bradford et al., 2018, section 4.3.1).

Shark-Management-Alert-in-Real-Time (SMART) drumline bycatch was routinely sampled as part of the shark release program. A SMART drumline is a modification of traditional drumline technology to include a SMART buoy that alerts a land-based team to the capture of an animal (Tate et al., 2019). The land-based team would then mobilise to release the animal from the SMART drumline, with a response time of approximately 30 minutes following notification. During the release, the animal was measured, a tissue sample taken, and other biological information collected. Tissue samples were preserved in a DNA stabilising solution.

Necropsied GNS were primarily animals captured in the NSW shark meshing program that died before they could be released. These sharks were transported to freezer facilities for storage until such time a necropsy could be carried out. At the time of necropsy, a small tissue sample was taken and preserved either by freezing, immersion in ethanol or another DNA stabilising solution. Vertebrae were also collected from a subset of these sharks and subsequently used in a study of the growth rings to assign an age (N. Otway, pers. comm.). Data on length and sex were recorded at the time of necropsy.

2.2.2 DNA extraction

Tissue samples were collected and stored in ethanol or RNALater until used. Approximately 20-30 mg of sample was taken for DNA extraction. Total genomic DNA was extracted using either a modified version of the CTAB protocol (Doyle & Doyle 1987) or following the standard protocol of the DNeasy Blood and Tissue kit (Qiagen Inc., USA: www.qiagen.com/). The quality of the DNA was determined by Agarose gel electrophoresis and samples with low molecular weight DNA were not used in further analyses. DNA samples were shipped to Diversity Array Technologies (DArT, Canberra, Australia) for sequencing.

2.2.3 SNP selection and genotyping

The nuclear genotyping was completed in two steps following a similar approach to that described by Feutry et al. (2020). Single nucleotide polymorphism (SNP) discovery was carried out using the DArTseqTM protocol and based on 94 samples from across the population's geographic range. Following QC analysis and suitability assessment for DArTagTM assay design, the 2800 SNPs with highest minor allele frequency, which maximised kinship inference power, were retained to develop a DArTagTM genotyping assay. All samples were then genotyped by Diversity Arrays Technology Pty Ltd using the species-specific nuclear DArTagTM assay.

The sex marker identified in the previous study was not captured in the DArTagTM assay; therefore, all samples were genotyped with the DArTseqTM protocol, and that marker was used to determine the sex of all individuals.

2.2.4 Mitogenome sequencing

Full mitogenome sequences previously obtained from 477 individuals (Bradford et al., 2018) were aligned revealing 175 variable sites and a new DArTagTM assay was developed specifically for these sites. Library preparation and sequencing for all samples was undertaken by DArT for the species specific mitochondrial DArTagTM assay. All reads from all samples with read depth > 7 and without homo polymer GGGGGGG were pooled. The first 15 bases of all reads, containing the oligo sequences, were trimmed. All reads were then aligned to the consensus (99%) of the 477 sequences given for design using minimap2 and 0% majority was used to call the alleles at each variable site identified during the design process. No new putative variable site was used in this analysis. Variable sites with missing data for one or more individuals were removed, resulting in 56 sites in total.

2.2.5 Growth curve

Given that CKMR uses information on the relative ages of two individuals, developing an Australian growth curve was a key component of the current project. Vertebral sections from 46 GNS with associated length measurements (provided by NSW DPIRD) were processed at the Central Ageing Facility.

To process the GNS samples, three vertebrae were cut from the frozen core. The tissue was carefully trimmed from each of the vertebrae using a scalpel. When most of the tissue had been removed, the vertebrae were immersed in a concentrated bleach with active ingredients being sodium hypochlorite (10%) solution and sodium hydroxide (1.3%). This bleaches the vertebrae and removes tissue inaccessible using a scalpel. Immersion times were 5-30 minutes depending on the size of the vertebrae being bleached. Larger samples require a longer soak time. After bleaching, the vertebrae were rinsed through a series of three water baths to remove all traces of the bleach solution and then oven dried at 55°C. The cleaned and dried vertebrae were placed in labelled envelopes until required for sectioning.

Vertebrae were then embedded in molds using a casting resin. These were dried and cut using a high speed isomet saw at ~300-400 microns. Sections were mounted on slides and cover slipped using the same casting resin. Samples were read using a Leica M80 with Rotterman contrast transmitted light and central ageing facility image software. There were also a number of known-age animals in the samples provided to assist in the identification of annual zones. This study followed the approach of Goldman et al. (2006) by looking for an annual zone.

2.2.6 Age-given-length uncertainty

Shark ageing from vertebral sections is known to be prone to significant uncertainty, especially in the older age classes, hence it is desirable to consider the uncertainty in the ages of each animal. Therefore, as an input into the CKMR models, estimates of the probability of age conditional on length were constructed.

This used an empirical Bayes approach in the following steps:

Estimate $\Pr(L|a)$ using length data partitioned into length-bins.

Estimate $\Pr(a)$ the prior distribution of age in the sample set.

Use Bayes Theorem to estimate $\Pr(a|L) = \Pr(L|a)\Pr(a)/\sum_a \Pr(L|a)\Pr(a)$.

For step 1, the support for the distribution of sample lengths from the sample as

$$l_{pred} = (min(L) - 1.96\hat{\sigma}, max(L) + -1.96\hat{\sigma})$$

was characterised to compute the distribution of age given a length class in l_{pred}.

$$\Pr(a|L) \sim \text{log-normal}\left(l_{pred}, \log\mathbb{E}(l|a), \sigma_{la}\right)$$

where parametric error from the Von Bertalanffy growth function (VBGF) estimates and stochastic error are combined into

$\sigma_{la} = \sqrt{SE_{l|a}^2 + \sigma_{la}^2}$.

To construct $\Pr(L)$ given $\Pr(L|a)$ and $\Pr(L)$ are estimated

$$\Pr(a) \propto \mathcal{N}\left(a_{pred}, \log\mu_{prior}, \log\sigma_{prior}\right)$$

Such that the prior is normalised to give $\Pr(a) = \Pr(a)/\sum_a \Pr(a)$

Finally, the negative log-likelihood of

$$\mathcal{L}_{prior} = \sum_a \text{multinom}\left(\hat{n}_l, N_{eff}, \hat{p}_l\right)$$

where $\hat{p}_l = \sum_{l_{pred}} \Pr(a|l) * p(a)$ is assumed.

2.2.7 Kinference

Acronyms:

FSP	Full Sibling Pair
GGP	Grandparent Grandchild Pair
HSP	Half Sibling Pair
POP	Parent Offspring Pair
SNP	Single Nucleotide Polymorphism
UP	Unrelated Pair

Sequenced data were cleaned by removing loci having low mean read depth across individuals and loci where the reference or SNP allele had a frequency of < 10% in the population. For some loci, 'null' alleles were present. Briefly, null alleles are assumed to result from mutations at restriction site for the locus, or from indels that change the length of the allele, causing it to not be recognised as the same locus. In either case, null alleles cause missing sequence data for that locus. Nulls are heritable and so are informative about kinship. For each locus, null allele frequency was calculated following Hillary et al. (2018). After accounting for null alleles, loci whose genotype frequencies were incompatible with Hardy-Weinberg Equilibrium were removed. Samples were checked using tests included in the R package *kinference* (Bravington et al., *in prep*). Samples were excluded if they showed outlying low genotype likelihood across all loci, given population allele frequencies for each locus (test 'ilglk_geno'), if their null allele and heterozygote frequencies showed evidence of cross-contamination or sample degradation (test 'hetzminoo_fancy'), or if they were a near-duplicate of another sample (test 'find_duplicates').

Kin-finding was performed using the R package *kinference* (Bravington et al., *in prep*) which calculates likelihood-ratio statistics for pairs of samples. Separation of kin-pairs into different kinship types was done using a series of 'PLOD' statistics. PLOD statistics are an odds-ratio statistic comparing the likelihood of observing pairs of genotypes if a pair truly is of a particular kin-type versus another kin-type (e.g., HSP vs UP). For separating kin that are known to be one of two particular kin-types (e.g., FSP or POP), the PLOD statistic built using those two kin-types is statistically optimal. The specific PLOD that uses half-sibling pairs and

unrelated pairs for its two odds-ratio components is the 'PLOD_HU' (i.e., PLOD, HSP/UP). Other PLOD statistics are named using a similar convention (e.g., PLOD_FP: FSP/POP). The PLOD_HU is a powerful general-purpose 'strength of kinship' statistic that is useful for sorting kin into first-order kinships, second-order and weaker kinships, and functionally-unrelated pairs.

First-order kin (POP, FSP) were split from all less related kin using the PLOD_HU statistic, which optimised for HSP/UP separation, but also separates first and second order kin (Figure 1, subfigure A). POPs were then separated from FSPs using the PLOD_FP statistic, which is optimised for FSP/POP separation. A mixture model was fit to the PLOD_HU distribution of kin pairs except POPs and FSPs, with separate mixture components for second-order (HSPs and grandparent-grandchild pairs, GGPs), third-order (e.g., full-cousin) pairs, and fourth-order (e.g., half-cousin) pairs (Figure 1, subfigure B). This mixture model was used to set a PLOD_HU threshold with a low false-positive rate of two expected false-positive HSPs. Pairs above the threshold were used as HSPs unless they were already included in the set of POPs or FSPs, and a false-negative rate for HSPs was estimated from the mixture model. This kin-calling approach groups GGPs with HSPs as they are not distinguishable using this method. The CKMR model applied to this data allows for both HSPs and GGPs (Bradford et al. 2018).

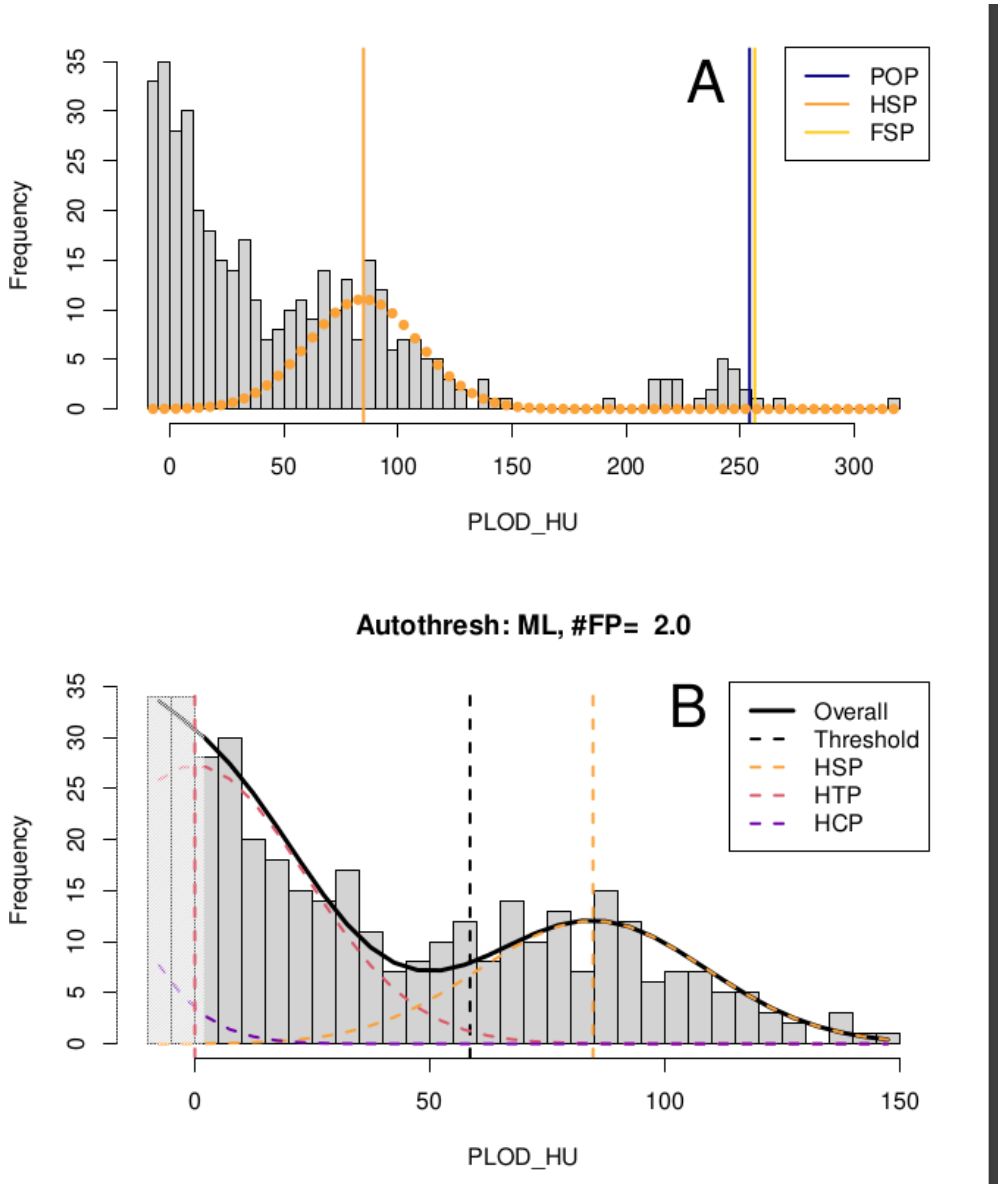

Figure 1: PLOD distributions and cutoffs in *kinference*. Subfigure A shows the PLOD_HU distribution for all pairs with PLOD_HU > -10, with expected mean PLOD_HU scores for POPs, FSPs, and HSPs given as vertical lines and inferred distribution of HSP PLOD_HU scores given points. The gap between first-order kin (POPs and FSPs) and second-order kin (HSPs) is clearly visible between PLOD_HU = 150 and PLOD_HU = 190. Subfigure B shows the mixture model of PLOD_HU scores for second- (e.g., HSP), third- (e.g., half-thiatic, HTP), and fourth-order (e.g., half-cousin, HCP) kin. The sum of these component distributions is given as a solid black line, and the cutoff for pairs 'called' HSPs is given as a dashed vertical line.

2.2.8 Close-Kin Mark-Recapture Model

The CKMR model by Bradford et al. (2018) was used. This model uses the same underlying population-dynamics model that was used for white sharks (Hillary et al., 2018b) but incorporating some structural changes to account for differences in life history and the available dataset. The differences in the CKMR model for GNS were described by Bradford et al. (2018). Briefly, the wide age range within the GNS dataset required a more elaborate

CKMR model than that used for white sharks to allow for more kinship possibilities (e.g. POPs and GGPs) and required us to assume that the age composition of adults had been stable for a relatively long period. The assumptions of the model are provided in Appendix A.

Central to CKMR theory is the identification of kin-pairs, which itself depends on accurate length measurements to assign an age to the sampled animal. In the current project, the measurement of sampled animals was improved over the previous project by using stereo imagery. Despite this, there were instances where an accurate measurement was not possible; therefore, uncertainty is allowed for in all length data. As before, the length data were grouped into three categories based on how reliably length was estimated a CV was assigned to each category: measurements made by eye (10%); stereo camera measurements (5%); and biopsy samples (1%).

A range of age-at-length scenarios were trialled. Initially, the close kin model was applied to the new sample data using the growth curve of Goldman et al. (2006) to provide a direct check and comparison to the output reported by Bradford et al. (2018). This was switched to the new curves described in section 2.3.1 that estimate length-at-age from Australian data for both sexes combined. It is known that age estimates from vertebral ageing are likely to be biased downwards for mature individuals (Passerotti et al., 2014), which would result in a growth curve that suggests faster growth than reality (because animals will appear to achieve their maximum length at a relatively younger age). To investigate the impact of such a bias on the results of the close kin model, a growth curve that has slower somatic growth was used by reducing the K parameter value of the von Bertalanffy growth curve (and consequently increasing the t_0 parameter value) with the length at age zero and the asymptotic length L_{inf}, both unchanged.

Age-at-maturity (a_{mat}) for Australian GNS is uncertain, therefore, two scenarios were used. These scenarios are the same as those used by Bradford et al. (2018) to allow for direct comparison. These were based on published reports (Bass, et al., 1975; Gilmore et al.; 1983; Branstetter & Musick, 1994; Lucifora, et al., 2002; Goldman, et al., 2006). The two scenarios are: *High* a_{mat} and *Low* a_{mat}, age-at-maturity 14, 11 (F, M) and 10, 7 (F, M) respectively (Appendix C).

Appendix B outlines the population dynamics equations and probabilities of the CKMR model used (reproduced from Bradford et al., 2018).

2.3 Results

2.3.1 Growth curve

Age estimates were obtained from vertebral sections from 46 GNS. Their estimated age ranged from 1 to 19. The length range was 1.5-3 m TL. The resulting VBGF model estimates are shown in Table 3 and the fit to the observed data is given in Figure 2. Visually, the fits appear adequate, and the uncertainty estimates (Figure 3A) indicate low CVs over the range (mostly less than 5% up till around age 20). Given longevity estimates of species (30+ years), this data does not encompass older individuals. However, the reliability of vertebral sections for ageing mature individuals is also less certain.

A standard Von Bertalanffy growth model was used to model length-at-age:

$$\mathbb{E}(L_a) = L_\infty\left(1 - e^{(-\kappa(a-t_0))}\right)$$

Where $\mathbb{E}(L_a)$ is the expected length at age a , L_∞ is the asymptotic maximum length estimate, κ is the growth rate parameter and t_0 is the theoretical age where size is 0. The

model was fit via maximum likelihood using the *TMB* package in R. We assumed that errors on ageing data are log-normally distributed.

$$\mathcal{L}_{VB} = -\sum_{i=1}^{n} \log \mathcal{N}\left(L_i, \log\left(\mathbb{E}(\mathbb{L}_{a_i})\right), \log(\sigma)\right)$$

The R *TMB* package uses the Delta-method to estimate the uncertainty on model predictions and, therefore, give an error and coefficient of variation on length at age. We also examined the coefficient of variation on predicted Length-at-age from the log-normal distribution using the fact that for log-normal random variable X, $CV(X) = \sqrt{\exp(\sigma^2) - 1}$ where σ is the variance of X.

Table 3. Parameters of the Von Bertalanffy growth model.

	Estimate	Std Error
L_{inf}	2.978	0.066
K	0.161	0.014
T_0	-2.484	0.213
L_{sigma}	-2.605	0.074

The distribution of length conditional on age (Figure 3A) reflects the VBGF fit uncertainty, with reduced uncertainty up till the maximum age in the data and considerable uncertainty for older ages. This is bounded below (e.g., a 3 m shark has a considerable chance of being older than 20 years, but a very low chance of being younger than 20 years). The distribution of lengths in the sample (used in the construction of the age prior) is shown in Figure 3B, highlighting the reduced number of small individuals and maximum size of 3 m.

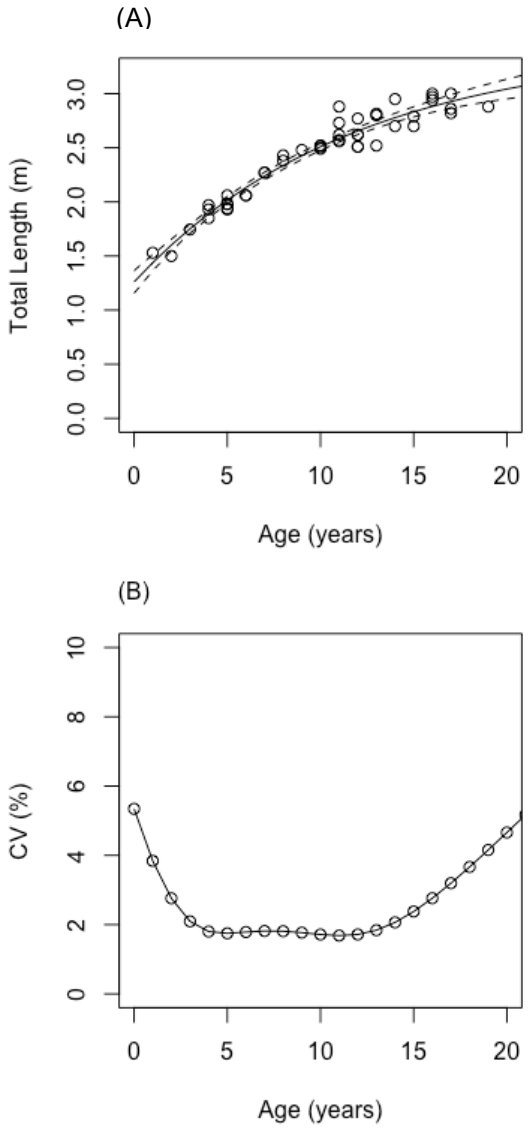

Figure 2. (A) length at age observations and estimated VBGF function (with SEs). (B) The coefficient of variation on estimates of length-at-age.

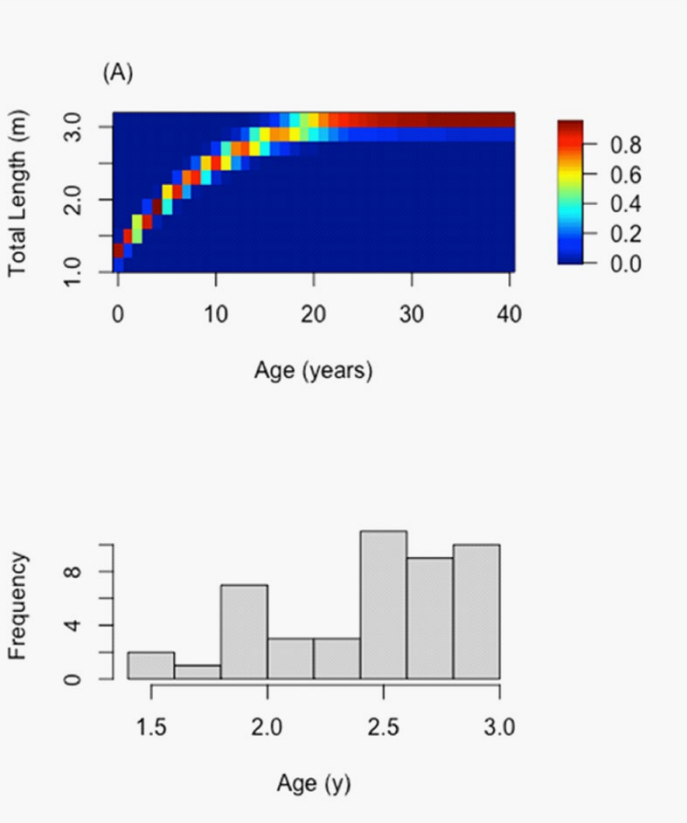

Figure 3. Probability of length conditional on age. (B) Age distribution of data to inform the range of length bins used to generate P(a/L).

The estimated parameters of the prior lognormal distribution were $\log\mu_{prior}$ = 2.21 and $\log\sigma_{prior}$ = 2.2 resulting in the prior age distribution shown in Figure 4.

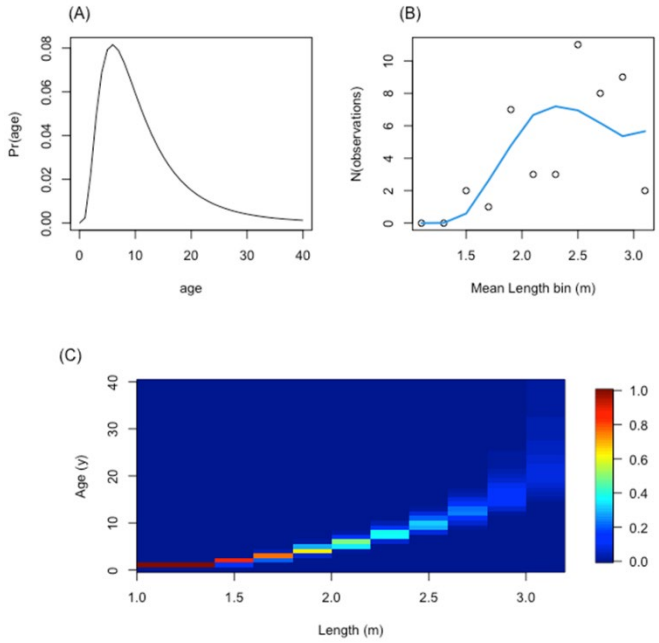

Figure 4. (A) Estimated prior distribution of ages (B). Fit to length data. (C) Probability of age conditional on length.

2.3.2 Kinference

A total of 272 GNS were biopsied by SCUBA in 2023. Of these, 21 biopsies failed to collect a sufficient tissue sample. A further 100 GNS caught and released through the NSW SMART drumline program were biopsied. A single tissue sample was provided by Northern Territory Fisheries. To supplement this dataset, 31[2] DNA samples collected from the previous GNS CKMR project (Bradford et al., 2018) were included in the material (376 samples) sent to DArT for sequencing. Total length (natural) ranged from 1246 to 3600 mm (average = 2400.9, SD = 359.8 mm). The sex ratio of the samples included in the final analysis (i.e., those not excluded on genetic grounds or missing crucial metadata such as length or year of capture) was 64% female.

Sampling was spread across 32 different sites in NSW (Figure 5) and one site each in the Northern Territory and Victoria. Despite the wide geographical spread of sampling, eight sites contributed 71% of all samples used to estimate GNS abundance.

[2] The full dataset used for the 2018 abundance estimate was not used in the current analysis because of inaccurate length measurements.

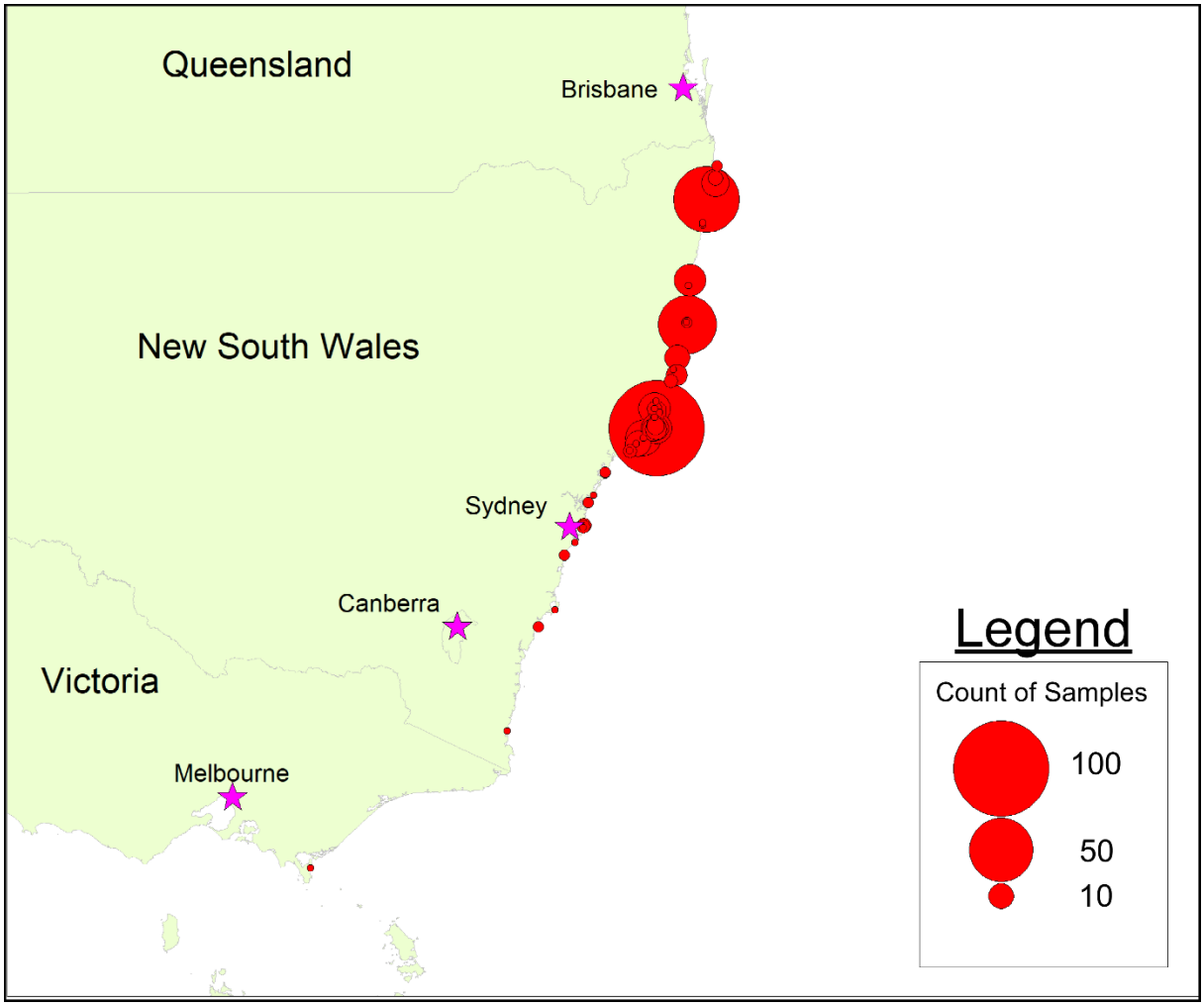

Figure 5. Thematic map highlighting the spread of sampling effort.

2.3.3 Close-Kin Mark-Recapture Model

Using the new dataset and an Australian growth curve, adult abundance in 2023 was estimated at 1,423 (CV = 0.18) adults (Table 4), with an estimated annual rate of increase of 5% (2.3-7.1%, 95% CI). Similar results were observed under the scenarios of a fixed t_0 and sex specific growth curves (Table 4). The full model output is provided in Appendix C.

Table 4: CKMR output with a growth curve estimated from Australian GNS and age at maturity set to 10 years for females and 7 years for males. N_{xxxx} is the adult population in year xxxx. (1) "New laa" uses a single growth curve calculated from combined male and female samples with t_0 estimated.

Model Scenario	N_{1975} (95% CI, *CV*)	N_{2017} (95% CI, *CV*)	**N_{2023}** (95% CI, *CV*)
[1]New laa	129 (0 - 266, *0.54*)	1054 (744 - 1364, *0.15*)	**1423** (921 - 1925, *0.18*)

The new set of samples (*New samp,* Appendix C), with improved kin finding and more accurate length measurements, approximates the observed numbers of kin pairs more closely than when the older dataset was used (see Appendix C). Note that the USA growth curve was still used for this scenario. When the growth curved based on Australian age and length data (for both sexes combined) was used, the match between observed and model expected numbers of kin pairs was greatly improved (*Aus laa,* Appendix C).

Setting the value for t_0 for the growth curve to the value from Goldman et al. (2006) to ensure that the length at age zero was more realistic, had minimal impact on the results of the close kin model (*Fix* t_0*,* Table 4).

There were insufficient data for males to allow estimation of all three parameters of the von Bertalanffy growth curve, but when t_0 was fixed, sex specific growth curves could be estimated. The curve for males should be regarded with caution as it was based on just 13 samples. The close kin model results for this scenario (*Sex laa,* Table 4) are very similar to those estimated from a single sex aggregated growth curve.

Slowing the rate of growth in length-at-age by reducing the von Bertalanffy *K* parameter to two thirds of its estimated value, increased the estimated rate of population growth to 8% p.a. (*Slow K,* Appendix C). The fit to the data, however, was worsened (the negative log likelihood is larger). As the change in rate of somatic growth was made arbitrarily to investigate what direction the close kin results would change, this scenario should not be treated as indicative of reality except to note that the current estimate of population growth rate could be biased downwards if vertebral ageing underestimates the age of older sharks, as shown by Passerotti et al. 2014.

Correcting the allocation of uncertainty (CV) to the three length precision categories, while still using the 2018 dataset, resulted in a large increase in the estimate of population growth from 3.4% to 6% (*Rev len CV,* Appendix C).

2.4 Discussion

Close-Kin Mark-Recapture is premised on being able to determine the relationship between pairs of sampled individuals. Specifically, whether the pairs are parent-offspring, full sibling, half sibling, or more distantly related pairs. To achieve this, it is important to obtain accurate length measurements to be used in conjunction with a growth curve to infer the age of the sampled individual. Unlike the previous CKMR abundance estimate for adult GNS (Bradford et al., 2018), the current project has a high proportion of accurately measured individuals, resulting in a better resolution of the relationship between sampled pairs.

Uncertainty in age estimates results in bias for CKMR models (Petersma et al., 2024), such that underestimating age negatively biases population abundance estimates. A growth curve is used to infer length from age; however, as growth may differ between populations, it is important to use an appropriate growth curve for the population in question. In the previous GNS abundance investigation (Bradford et al., 2018), age was inferred using a growth curve derived from data collected in the USA. For the current project, an Australian GNS growth curve was available which has achieved a much closer match between observed and expected numbers of kin pairs.

The effect of applying an inappropriate growth curve is illustrated in Appendix C where the match between observed and expected numbers of kin pairs is poor when using the USA growth curve on the new dataset, as well as when the growth curve was deliberately altered to explore the impact of downward bias in ageing of older sharks.

Using the species-specific DArTagTM assay coupled with a refined kin-finding process has greatly improved the ability to identify the level of relationship between kin pairs.

Consequently, the discrepancy between observed and expected kin pairs identified in Bradford et al. (2018) has been resolved such that the model now reproduces these numbers almost perfectly.

Adult abundance in 2023 for the eastern Australian GNS was estimated to be approx. 1,420 individuals (range: 921 – 1925, Fix t_0) with growth estimated to be 5% (range: 2.3 – 7.1%) per annum. The abundance estimate from the current study is slightly less than reported in Bradford et al. (2018); however, the annual rate of increase is higher.

An error in the assignment of uncertainty in length measurements by Bradford et al. (2018) was identified when checking the CKMR model. This had the potential to bias age estimates and hence abundance and trend. Rerunning the CKMR model with all parameters as previously but correcting the length uncertainty lowered the 2017 abundance estimate (Appendix C: *New samp with USA VB*).

Petersma et al. (2024) detailed how using an inappropriate growth curve has the potential to bias age assignment with a flow-on impact when estimating abundance using CKMR. The USA growth curve, when used in the new analysis, returned a higher abundance and rate of increase than when using the Australian growth curve, highlighting the importance of using a species-population-specific growth curve.

3. Estimates of age dependent survival in *Carcharias taurus* from acoustic telemetry

3.1 Introduction

Survival rates are fundamental in structuring populations and determining their productivity and recovery following depletion. Estimating survival rates with respect to age, sex or other demographic groupings, either requires the ability to know the fate of a representative sample of individuals or collect data of their life status through time - otherwise known as a capture or resight history.

Obtaining data to estimate survival in wild populations is generally challenging and time/labour intensive. In some rare cases, known-fate data are available but capture history data are more common. Marine species often present further challenges due to inaccessibility, inability to reliably identify individual animals easily, or monitor habitats for long periods visually for the presence of individuals. For some marine species, tagging with dart tags, or the ability to recognise individuals from markings can be used to form capture histories.

Acoustic telemetry arrays can also generate these series (Dudgeon et al., 2015, Lees et al., 2021) which have been used to estimate survival rates in various species. It is recognised that these methods have potential for bias (Peterson et al., 2021) due to problems with sample size and receiver/array design. In many, if not the majority of studies, design testing is not carried out ahead of deployment of tags, making it hard to diagnose whether biases exist in a particular study.

Several Australian research agencies and institutions have fitted GNS with long-term acoustic tags at various sites around the Australian east coast. These data, therefore, contain some signal on apparent survival rates. Unfortunately, with these data it is not possible to distinguish if non-detection is the result of the death of an animal, or if the animal is alive but has moved away from a location covered by acoustic receivers, or if the tag has failed. However, the data can be used to estimate a detection probability (see methods below). This study accessed acoustic telemetry data from the Australian Integrated Marine Observing System (IMOS) for "*Carcharias taurus*" and attempted to estimate age-dependent survival rates accounting for detection probability.

From the outset, there are limitations to be acknowledged in these data for the purpose of estimating survival. Firstly, the number of tagged animals was not large, consisting of 72 animals tagged between 2011 and 2023. Of these, 17 were missing deployment details and a further 12 had no associated length data. This left a total of 43 tagged animals that could be used in this analysis. Second, the detection of individuals is heavily influenced by the design of the array, and this influences the ability to estimate survival (Patterson and Pillans 2019). Finally, estimation of survival was not the primary objective of the individual studies which generated these data, and the deployments were not, for instance, spread across ages and sexes. These factors immediately indicate limitations which cannot be overcome easily. Nevertheless, the data set spans over a decade and consists of many juvenile animals, making it a worthwhile set of observations for considering survival in this Critically Endangered population.

Given the longevity of the species, low abundance and low reproductive output, for GNS populations to persist, survival rates of individuals are likely to be high - even for younger age classes. This is especially the case given the known reproductive output of females having only at most two pups every other year.

Several studies have produced survival estimates for GNS in Australian waters and globally. However, there has been considerable variation in how these estimates were compiled. Given the lack of informative data, Otway et al. (2004) modelled survival as a function of maximum lifespan ω (taken to be 25 years); the natural mortality rate (M) was taken as M=-ln(0.01)/ω. This study, therefore, assumed that 1.0% of the individuals remain at age ω. This resulted in a constant value of annual survival (e^(-M)) of 0.83 per year. Bradford et al. (2018) using CKMR data, directly estimated adult survival rates to be 0.95-0.97 per year. However, CKMR does not inform on juvenile survival. Estimates from an integrated population model in South Africa (Dicken et al., 2008) suggested reasonably high survival for adults (0.89 pa) and quite low in juveniles (survival = 0.56 pa)

In this study, acoustic telemetry data has been used to inform a model of age-dependent survival and also estimate observation probability. As noted above, the model is based on a small data set of tagged individuals which carry long term (~10 year) tags and also have size data which was used to estimate age at tagging.

3.2 Methods

Acoustic detection data was downloaded from the IMOS Animal tracking facility (ATF) databases, along with meta-data on release date, size and sex. In this study, data from two NSW acoustic tagging programs that had available size data, from which age could be estimated (using the growth model shown in section 2), were used. The raw detection data were compiled into an annual capture history matrix $Y_{k,t}$ which details whether the k-th animal was detected in year t

$$Y_{k,t} = \begin{cases} 1 & \text{if } k \text{ detected in year } t \\ 0 & \text{otherwise} \end{cases}$$

The capture history data were used in a Cormack-Jolly-Seber (CJS) model fitted as a Hidden Markov Model (Laake 2013) with a continuous covariate (King and Langrock 2016). The model estimates the annual survival as the transition probability $\phi_a$between two possible states (Alive and Dead) dependent on age a_t, which is calculated from an initial estimate of size at tagging and time elapsed to the next capture.

$$\Pr(S_{k,t}|S_{k,t-1}) = \begin{pmatrix} \phi_a & 1-\phi_a \\ 0 & 1 \end{pmatrix}$$

Here we model age dependent survival as a logit-linear function

$$\phi_a = \text{logit}^{-1}(\beta_0 + \beta_1 a_i)$$

where a_i is the estimated age at tagging of the ith animal, β_0 is the intercept parameter and β_1 the slope, on a logit scale.

We assumed a constant, average detection probability p so that the data likelihood is given by:

$$Pr(Y_{k,t}|S_{k,t}) = \begin{cases} p & \text{if } Y_{k,t} = 1 \\ 1-p & \text{if } Y_{k,t} = 0 \end{cases}$$

These were fitted within a Hidden Markov Model following King and Langrock (2016) where the negative log likelihood is given by

$$\mathcal{L}_t = \delta_0 \sum_i \sum_t \ln \Pr(S_{k,t}|S_{k,t-1}) \Pr(Y_{k,t}|S_{k,t}) \quad (\#Eqn\ NLL)$$

Here the initial state probabilities are $\delta = (1,0)$ - i.e., all individuals start as alive. Maximum likelihood estimates were obtained by standard numerical minimisation of EqnNLL. These estimates were used as the starting values for a Metropolis-Hastings (MH) algorithm which

allows for calculation of posterior distribution on the survival rate as a function of age. The proposal distribution for the Metropolis-Hastings Markov chain Monte Carlo (MH-MCMC) runs was $\theta^* \sim \mathcal{N}\left(\hat{\theta}, \mathbb{H}(\hat{\theta})^{-1}\right)$, where $\mathbb{H}(\hat{\theta})^{-1}$ is the inverse-Hessian matrix from the Maximum Likelihood Estimation (MLE) fits. We also assumed priors on model parameters as $logit\ p \sim \mathcal{N}(0,0.5)$, $logit\ \beta_0 \sim \mathcal{N}(0,1)$, $logit\ \beta_1 \sim \mathcal{N}(0,1)$. The MH algorithm was run for 50,000 iterations with multiple randomised starting values. Gelman-Rubin statistics were used to assess convergence over three MCMC chains.

3.2.1 Demographic estimate of early survival

The telemetry data does not cover the age range from 0 to the minimum size/age at tagging (this was approximately 4 years old). However, by combining knowledge of GNS demographics and the estimates from the CKMR, a minimum survival rate over these years can be estimated that would be consistent with the other results. The estimates also assume that the population has a stable age structure.

The CKMR provides estimates of adult abundance N_A, sex ratio (ν) and population growth rate (λ). We know also that female age at maturity is expected to be age 10 and that females have two pups every other year (and thus annual average pupping rate is one per female).

This allows us to form β_f - expected reproductive output at age. It also means that the expected number of pups produced per year is equivalent to the number of females, since on average, we expect a pup from every female.

Let ϕ_n be the survival from age 0 to the minimum age in the tagging data ($\min(a_tag)$). Then we model the transition from ϕ_n to ϕ_a (from the CJS model above) as

$$\phi_a^f = \phi_j \xi_f + (1 - \xi_f)\phi_a$$

where,

$$\xi_f = \begin{cases} 1 & \text{if } a < \min(a_{tag}) \\ 0 & \text{otherwise} \end{cases}$$

(where minimum age at tagging a_{tag} =4).

To calculate the stable age distribution the cumulative survival to age a is required, given by

$$\ell_a = \prod_{i=0}^{A_{max}} \ell_{a-1}\, \phi_a^f$$

Based on these inputs, standard numerical methods were used to find the value of survival ϕ_n for animals aged 0 to $\min(a_{tag})$ such that the following holds true.

$$\nu_f \sum_a \ell_a \exp(-\lambda a)\beta_a = 1 \qquad (\#Eqn\ 2)$$

where, λ is the growth rate from the CKMR and β_a is reproductive output at age a (in this case 1 if $a \geq 10$ for females, otherwise 0). This solution for ϕ_n provides an estimate of the expected average survival from birth to the age of first estimates of survival in the CJS model. Which is then followed by the adult survival estimate ϕ_A from the CKMR modelling for ages older than the age of maturity. To obtain an estimate of uncertainty on ϕ_n, equation 2 is solved for each draw from the posterior distributions of β_0 and β_1 and used a 20% CV on the estimate of ϕ_A (0.95-0.97, Bradford et al., 2018).

3.3 Results

Data from tags deployed throughout the years 2011-2023 were used in this study. The bulk of the deployments occurred between 2016-2018 (Table 5) and this study used data from 43 GNS. Detections rose steadily from first tagging in 2011, peaking in 2017 (Table 5). In total, 763,232 detections were used to compile the annual capture histories used for survival rate estimates.

Table 5. Tag deployments and detection counts by year and program.

Year	GNS Monitoring		NSW DPI SEACAMS	
	Tags	Detections	Tags	Detections
2011	0	0	1	0
2012	0	0	0	0
2013	0	0	0	40
2014	0	0	0	15
2015	1	155	0	0
2016	2	19,485	4	4,400
2017	6	541,604	0	49,607
2018	13	84,742	0	5,944
2019	2	12,132	0	5,344
2020	0	13,785	0	3,560
2021	0	14,396	0	2,658
2022	8	2,322	0	172
2023	3	2,871	0	0

There were 14 females, 23 males and 6 animals where the sex was unknown. Based on the small sample sizes within sex, and since 15% of the animals were of unknown sex, no attempt was made at estimating sex-specific survival. The 43 GNS used in this study ranged in length from 1.91- 2.84 m with an average length of 2.3 m. The estimated age distribution (Figure 6A) shows that animals ranged in age from 4 to 16 years at first tagging (mean = 8). Detections were spread throughout eastern Australia from approx. -28 degrees in the north to -36 degrees in the south (Figure 6B). The annual capture histories (Figure 6C) had an average detection rate of 19.3% (range:7.7- 61.5%).

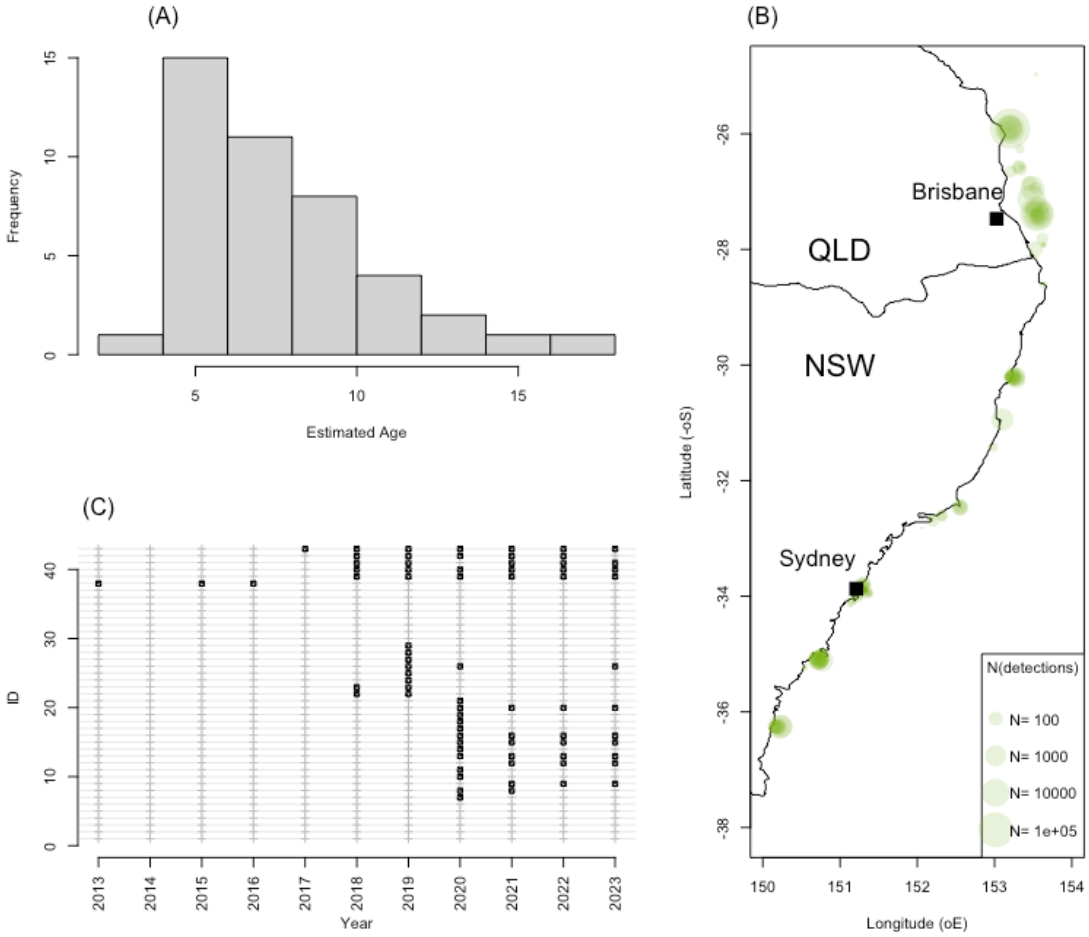

Figure 6. (A) Distribution of age-at-tagging estimates from lengths. (B) Map of acoustic detections of the tagged GNS used in this study. (C) Annual capture history for each of the 43 GNS used in this study.

3.3.1 Survival model parameter estimates

Geweke (1992) statistics on the Markov chain Monte Carlo (MCMC) analysis indicated no issues with convergence, and the last 25,000 values in the MCMC chain were retained after thinning to take every fifth value. This resulted in 5,000 values used to compute the posterior distributions shown in Figure 7. The posterior distributions departed substantially from the prior distributions, indicating that the data was informative in updating estimates of parameters (Figure 7).

Posterior means and credible intervals (CI) are given in Table 6. The estimated detection probability, p, indicated that there was a 42.8% probability of detection of a tagged GNS per year. The high value of the slope term ($logit^{-1}\beta_0 \approx 0.9$) indicated a high survival being estimated for even the youngest age class (around age 4). The small value of the slope (β_1) parameter indicated that the survival rate was estimated to increase relatively slowly with age, which was not surprising given the estimated high survival in the youngest observed animals.

The posterior prediction of estimated apparent survival at age is shown in Figure 8, which reflects the statements above; high survival in even the youngest animals and a slow increase in survival with age. The estimates are commensurate with the estimates of survival

in the breeding aged animals from the CKMR models (best estimate was phi_A=0.95, Bradford et al., 2018).

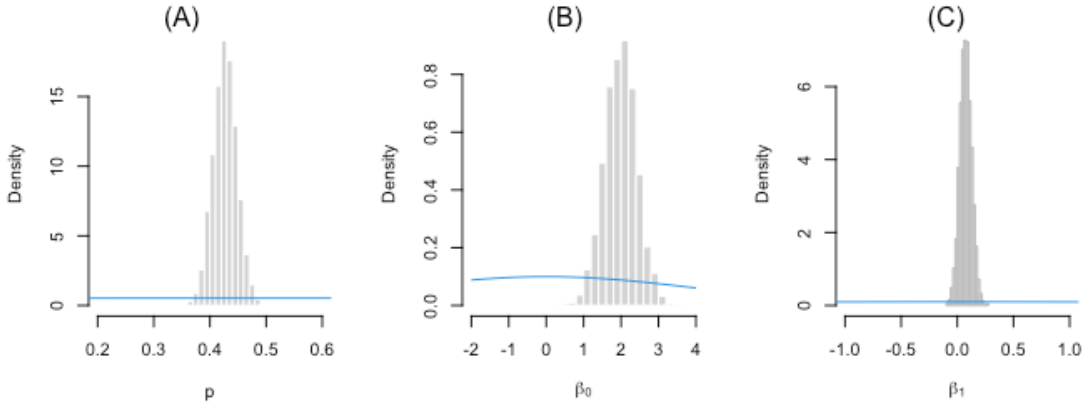

Figure 7. Posterior distributions for (A) Detection probability, (B) logit-intercept, and (C) logit-slope. The blue line in all panels shows the prior for that parameter.

Table 6. Posterior distributions for detection probability (P), logit-intercept (Logit-b_0), and logit-slope (Logit-b_1).

	Mean	lower 95% CI	Upper 95% CI
p	0.427	0.177	0.223
Logit-b_0	1.987	1.285	2.689
Logit-b_1	0.075	-0.010	0.165

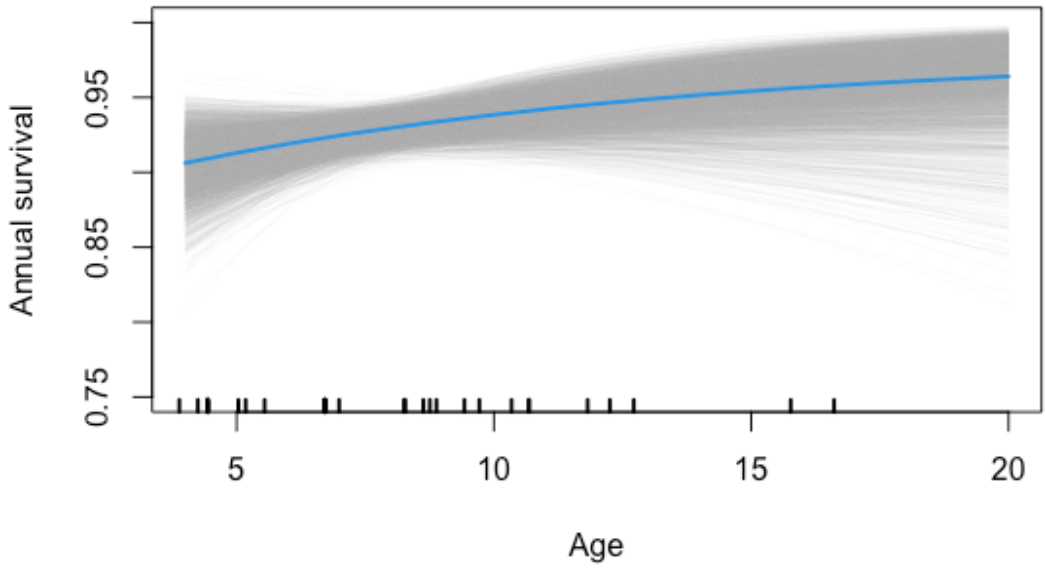

Figure 8. Estimated relationship of annual survival at age. The blue line shows the mean value, and the grey lines represent the posterior distribution. The rug plot on the x-axis shows the estimated ages at tagging of individuals in the study.

By combining life-history, estimated female abundance and population growth rate, age 0-4 survival was estimated to be 0.851 (95% CI 0.816 – 0.891) (Figure 9A). While less than survival for older ages, it still indicates that the life history of *C. taurus* dictates high survival from birth. Note that the younger age at maturity indicates that, given these estimates, males would have approximately three years with a few percent lower survival rates than females (Figure 9B).

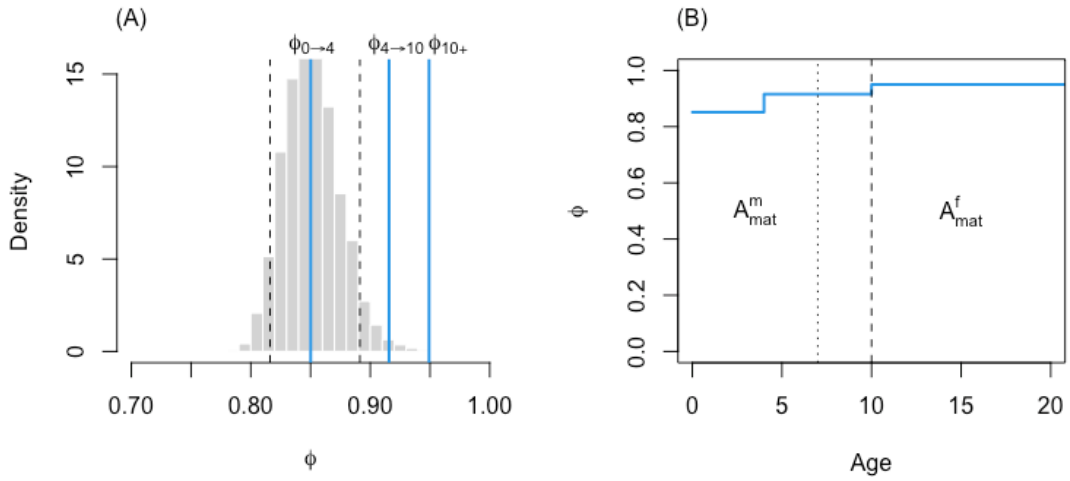

Figure 9. (A) Distribution of annual survival of age 0 to 4 year olds consistent with life history and CKMR results (histogram). Vertical blue lines give the mean survival estimated as: ‘n’ages 0-4; ’J’ ages 4-10; ‘A’ ages 10+. (B) Average survival at age for *C. taurus* using the averages over categories n/J/A. The vertical lines give the estimated age at maturity for males and females.

3.4 Discussion

The model shown here estimated plausibly high survival across the range of ages observed. However, there are caveats to note. This data represents a relatively small sample size from which to estimate survival rates. Nevertheless, the fact remains that the data collected from acoustic telemetry are one of few data sources available for estimating survival rates in GNS. The range of sizes used here covers a fair proportion of the estimated longevity of GNS (the maximum age attained by GNS is itself a poorly understood value). The data used here were dominated by male GNS (53% male, 33% female, 14% unknown sex), thus it is possible that it better represents male survival. This is difficult to tell from this model and further data would be required to shed light on how much survival rates may vary between males and females.

The data and method shown here indicated that GNS survival can be estimated from acoustic telemetry. The large number of detections for a modest sample size of animals likely reflects the species' tendency to spend long periods in known aggregation sites (where an acoustic array is most likely to be positioned). This site attached nature, combined with long life span, is likely to contribute to the estimated high detection probability, considering the large amount of coastal ocean used by the species.

By combining the survival estimates here with CKMR estimates of population size, growth rate, adult survival rates and sex ratio, it was possible to estimate a minimum average survival rate from neonate to the youngest age observed in the acoustic model. This was also relatively high. This points to high survival from birth being an integral part of the population's growth and viability in the face of low reproductive output.

The CKMR results (section 2) indicated a male-biased sex ratio (1.4:1 M:F. Appendix C, Table 8). While it was not possible to estimate sex-specific survival rates from these data, the general patterns of survival-at-age and differences in age-at-maturity were not sufficient to explain the adult sex ratio.

This study has not attempted to consider movement, but extensions of the CJS model to a multi-state model (Nichols et al., 1995; Lebreton et al., 2009) which explicitly estimates movement and survival rates at age may be possible. However, it is likely that such models would require larger sample sizes to parameterise with certainty.

4. Investigating epigenetic age of *Carcharias taurus*

4.1 Background

Individual age and age-class distribution are key variables behind understanding a variety of population parameters (Piferrer & Anastasiadi, 2023). However, obtaining accurate age estimates for aquatic species is time consuming and often requires lethal sampling methods. Consequently, this can be prohibitive when studying a listed threatened species such as the grey nurse shark (GNS).

A previous study aimed at obtaining an estimate of abundance for the Australian eastern GNS population (Bradford et al., 2018) used a growth model based on age-at-length of GNS from North America (Goldman et al., 2006). Following that study, the New South Wales Department of Primary Industries (NSW DPI) analysed the vertebral ring structure from 46 deceased GNS for which accurate length measurements were available. These data were provided to this study to develop a growth model specific to Australian GNS, and along with matching tissue samples, were also used to investigate the development of an epigenetic clock for GNS.

First developed in 2013 for use on humans (Horvath 2013), epigenetic clocks are a relatively new tool for the estimation of age. Epigenetic clocks calculate age based on methylation values at specific CpG (Cytosine-phosphate-Guanine) sites in the genome (Kabacik et al., 2022). Application of this technique to teleosts and elasmobranchs is still in its infancy, with the first scientific papers published in 2020 (Anastasiadi & Piferrer 2020; Mayne et al., 2020), and to date, has not been used on elasmobranchs. DNA methylation is a reversible process that may be influenced by environmental parameters such as heat stress (Drew 2022; O'Dea et al., 2016). It is, therefore, important to choose CpGs that are not influenced by factors other than age (Piferrer & Anastasiadi, 2023).

In the present study, a similar methodology to that which has been successfully used to build epigenetic clocks in fish, has been used to develop an age prediction model for GNS. This used conserved and previously identified age-associated CpG sites in school sharks (*Galeorhinus galeus*) to develop a multiplex PCR assay. This assay was carried out on 384 samples, of which 46 had vertebral age information.

4.2 Methods

4.2.1 Biomarker Identification

Potential age-associated cytosine-phosphate-guanine (CpG) sites were identified by performing a genome pairwise alignment between the previously developed school shark epigenetic clock CpG sites and the GNS genome (australasiangenomes 2023). The sites were targeted for primer design with PrimerSuite (Lu et al., 2017). A multiplex PCR assay was designed for one pool of primers targeting 21 CpG sites. One pool was designed, as this is the most cost-effective method for large scale processing.

4.2.2 Laboratory Work

In total, 392 samples were extracted for DNA using the Blood and Tissue Extraction Kit (QIAGEN). After extraction, eight samples were excluded due to low concentrations, resulting in a final set of 384 samples for downstream processing. All remaining samples were bisulfite treated for DNA methylation detection using an inhouse protocol. Potential age-

associated CpG sites were amplified using multiplex PCR where each pair of primers was tested individually with singleplex reactions. A total of 17 primer pairs amplified the correct target and were included in the final assay. Multiplex PCR reactions were barcoded with Illumina adaptors and pooled in equal volumes. The final library was sequenced on an Illumina Miseq.

4.2.3 Model Generation

Sequencing reads were aligned to the reference genome using Bismark (Krueger & Andrews 2011). DNA methylation values as a percentage were extracted from the sequencing data using Bismark's bismark_methylation_extractor function. Only 46 of the 384 total samples had associated age information and were, therefore, used to generate the epigenetic clock model. These samples were randomly subset into either a training set to calibrate the model, or a testing set to validate the performance. The model was calibrated by regressing the DNA methylation values from all CpG sites against natural log transformed age with an elastic net regression (Friedman et al., 2010). The glment R package was used to calibrate the model. The performance of the model was assessed by comparing the predicted ages to the vertebrate ages using Pearson correlations and absolute error rates.

4.3 Results

The model resulted in a poor correlation between the vertebral and predicted ages for both the training (Pearson correlation = 0.34, p-value = 0.46) and the testing (Pearson correlation = 0.25, p-value = 0.42) data sets (Figure 10A and 10B). Although the absolute error rate may be comparable to other studies, the overall error was high (Figure 10C). For example, samples < 5 years of age were predicted as 10-year-olds. Other iterations of the model resulted in a high performance for the training data set (Pearson correlation > 0.8, data not shown), however, this was not maintained in the testing data set (Pearson correlation ≈ 0.2), suggesting the model was being overfitted.

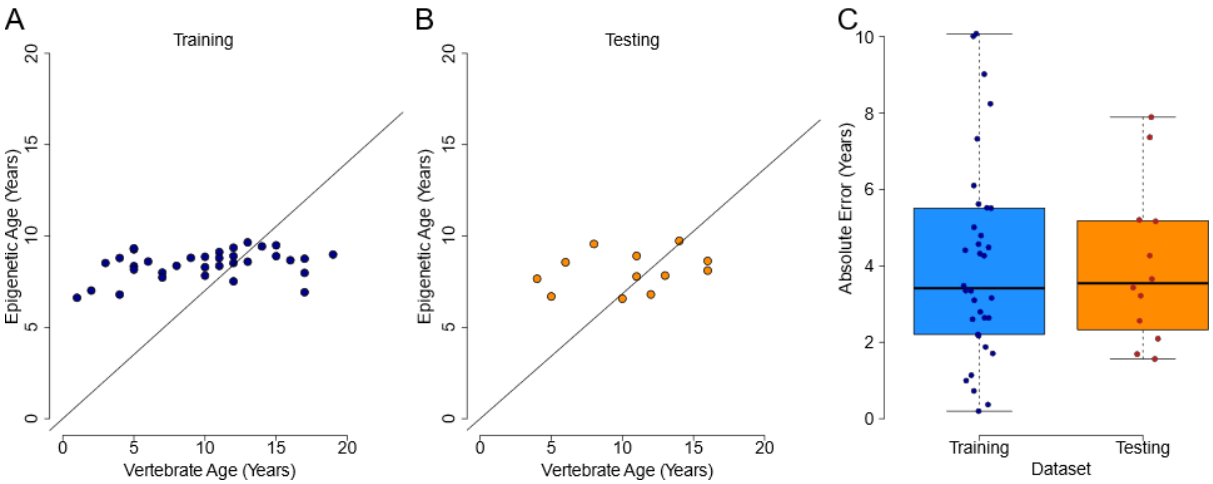

Figure 10. Epigenetic clock model of grey nurse shark. Correlation plots of the vertebral ages and epigenetic age predictions in the training (A) and testing (B) data sets. The model showed poor performance of age prediction across all age groups. (C) The absolute error in both training and testing data sets.

4.4 Discussion

In this study, we evaluated whether previously identified age-associated CpG sites in the school shark genome that are present in the GNS genome could be used as a GNS epigenetic clock. Unfortunately, these sites were not found to be age-associated in GNS. This could indicate the epigenetic clock for school shark is not conserved in sharks more broadly, but aspects of the current study limited our power to detect an age-related methylation signal.

The number of GNS samples for which vertebral ages were available was small and fell below the previously recommended minimum of 70 individuals to derive an epigenetic clock with appropriate accuracy and precision (Mayne et al., 2021). Ideally, the sample size would exceed 200 known age individuals (B. Mayne pers comm.). In addition, for calibration, the estimated age of samples should be within 20% of the actual age (e.g. for an animal that is 1 year old, the estimated age should be between 0.8 and 1.2 years).

In addition to small sample size, the choice of tissue and location of tissue collection can influence the derivation of an epigenetic clock (Bell et al., 2019). Ideally, tissue should be collected from the same part of the body for every animal sampled. For this study, information was not available on the type of tissues used for the extraction of genetic material (e.g., tissue is commonly collected from fins, muscle, connective tissue and internal organs) and this may have had an impact on the model.

Although age-association was not found, the remaining DNA methylation data generated in this study could potentially be paired with other phenotypic information, such as close-kin mark-recapture, to generate useful information for wildlife management.

It is probable that age-associated loci do exist for GNS and that examination of a broader range of loci would have resulted in the discovery of suitable epigenetic markers for ageing. The loci that were used, while providing a passable epigenetic clock for school shark, were not as tightly associated with age as they are for all teleosts examined. Better loci, selected specifically for sharks, would be of great value.

5. Origin of Northern Territory *Carcharias taurus*

5.1 Introduction

There have been several sightings and reports of GNS in waters off the Northern Territory and Timor Sea (Conoco Phillips Australia 2017; Momigliano & Jaiteh 2015). It is unknown whether these GNS are from the eastern Australian, Western Australian, or an unidentified population. During this study, a small number (N=2) of tissue samples were available for genetic examination. The aim was to try to determine whether GNS in NT waters were part of the Eastern or Western Australian populations, or potentially whether there was evidence of a third population. Given the very small sample size available to this study, these results can only be considered as a preliminary exploration, and further samples will be required to resolve the provenance and structure of GNS in NT waters.

5.2 Methods

Two tissue samples from GNS caught in Northern Territory waters were obtained for inclusion in the current analysis.

Sample from NT Fisheries.

This tissue was frozen for preservation providing the greatest opportunity to be able to extract high quality DNA. Location: -10.4 & 129.85 (Figure 11: NT GNS), date August 2016. Length and sex unknown, likely juvenile.

Sample from Museum and Art Gallery, NT. (NTM S.11791-001)

This tissue sample was from a formalin-fixed specimen with a lower probability of being able to extract suitable quality DNA for further analysis. Accession number: NTM S.11791-001. Location: Lynedoch Bank, Arafura Sea (-9.655 & 131.75) (Figure 11: NTMAG GNS). Initial attempts to extract DNA from this sample failed; there was very little DNA extracted with indications of contamination (F. Devloo-Delva, pers comm.).

Known-origin samples from both eastern and western Australian populations, and the single sample from the animal captured in the Northern Territory were available for comparison. The Northern Territory sample was compared to all other samples in the kinference dataset (data presented in section 2), comprising mostly eastern-origin animals. These samples were subjected to a series of tests using CSIRO's in-house kin-finding R package kinference (Bravington et al., in prep.) that looked for evidence of sample degradation and sample cross-contamination and the potential for the NT sample to cluster with animals from other populations. This test used population allele frequencies estimated from all samples in the dataset to determine whether a particular sample has allele frequencies that would point towards a different population of origin.

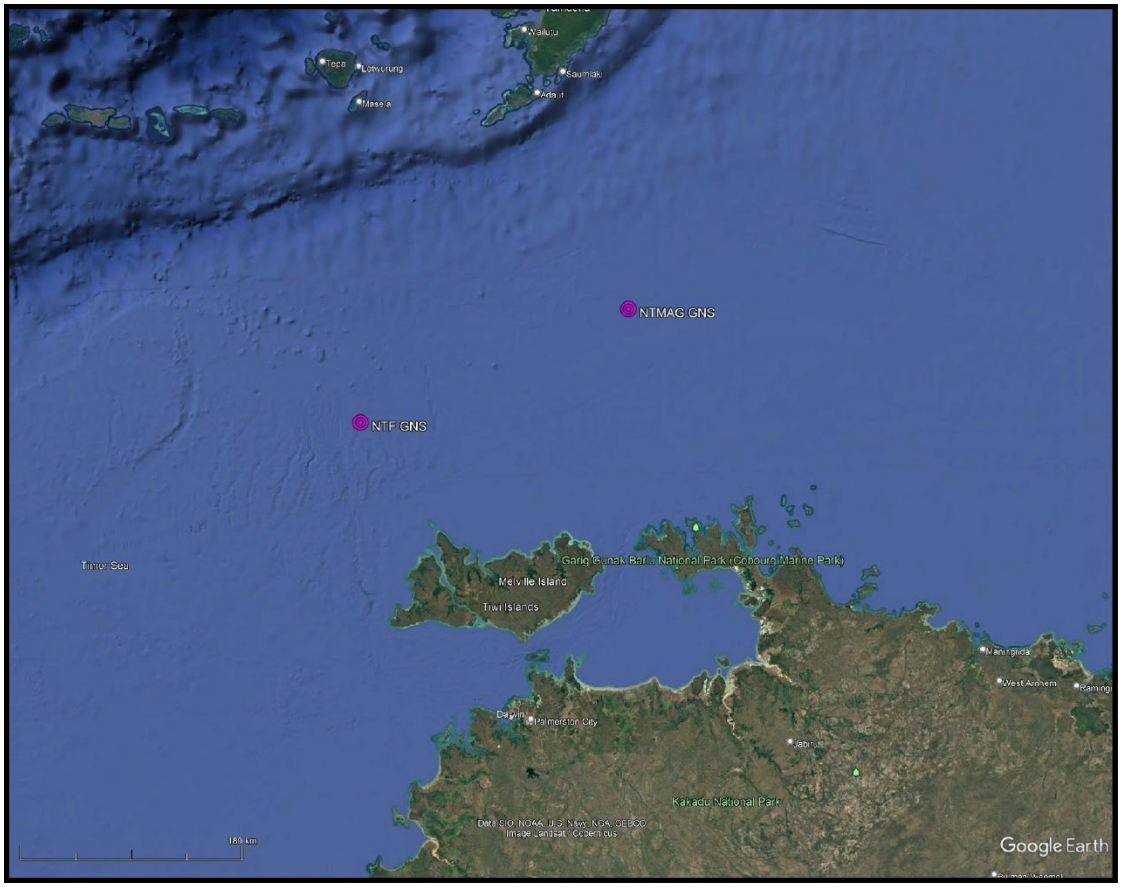

Figure 11. Location of grey nurse shark samples from Northern Territory waters.

Investigating the source population for the NT sample was carried out using a smaller, targeted dataset comprised of 44 eastern population GNS samples (including one from Victoria) and 19 known western population GNS samples. As was done with the larger kinference dataset (section 2.2.7), the smaller dataset was subjected to the same preparation and cleaning protocols. However, unlike the kinference dataset, provenance was genotyped to 'ABCO'[3] genotypes with the three most frequently observed sequence variants at each locus, in addition to the null allele, retained. Population allele frequencies were estimated separately at each locus for the NSW-sourced samples and WA-sourced samples. The allele frequencies for these two populations were used to inform a genotype likelihood-ratio test for East vs. West population membership given observed genotypes at each locus and the estimated population allele frequencies at those loci. This classification statistic was calculated for all samples, including the NT and Vic sample.

[3] In 'ABO' genotypes (kinference), 'A' denotes the most common sequence variant at a locus, and 'B' denotes any less-common sequence variant at that locus. Considering the two copies of each locus, there are four possible genotypes: AA if only the most-common variant is observed, AB if two variants are observed, BB if only a less-common variant is observed, and OO (null) if no sequence is observed. In 'ABCO' genotypes (provenance), 'A' and 'B' donate the most-common and second most-common variants, and 'C' denotes any sequence less common than 'A' or 'B', giving six possible genotypes: AA, AB, AC, BB, BC, CC, and OO (null). The genotypes are similar to those for ABO genotypes: AA if only the most-common variant is observed, AB if both the 'A' and 'B' variants are observed, AC if both an 'A' variant and a 'C' variant are observed, and so on.

Owing to small sample sizes of known-origin NSW and WA fish used to estimate allele frequencies for the two populations, we expect some ascertainment bias in this classification statistic. Ascertainment bias occurs for small sample sizes because population allele frequencies are estimated with low precision at each locus, but the estimated population allele frequencies exactly match their frequencies in the samples used to estimate them. Therefore, samples truly from the western population, but not included in the samples used to estimate western allele frequencies, are expected to show a bias towards zero in their likelihood ratio values. The same bias theoretically occurs for eastern samples as well, but the bias is expected to be smaller because of the larger sample size of eastern fish and, therefore, higher precision of eastern population allele frequencies. Ideally, this bias can be controlled by using a separate 'training set' of samples within each population to estimate the population allele frequencies, and a 'testing set' of samples to test the unbiased statistical power of the likelihood ratio test. In this study, a training set / testing set structure was not used as there were too few western samples to reserve some for the testing set and still have a reasonable estimate of population allele frequencies.

5.3 Results

The known-origin NSW and WA samples were cleanly separated by the likelihood-ratio test. Further, the Victorian sample clustered with the NSW samples, while the NT sample clustered closest to the WA samples (Figure 12).

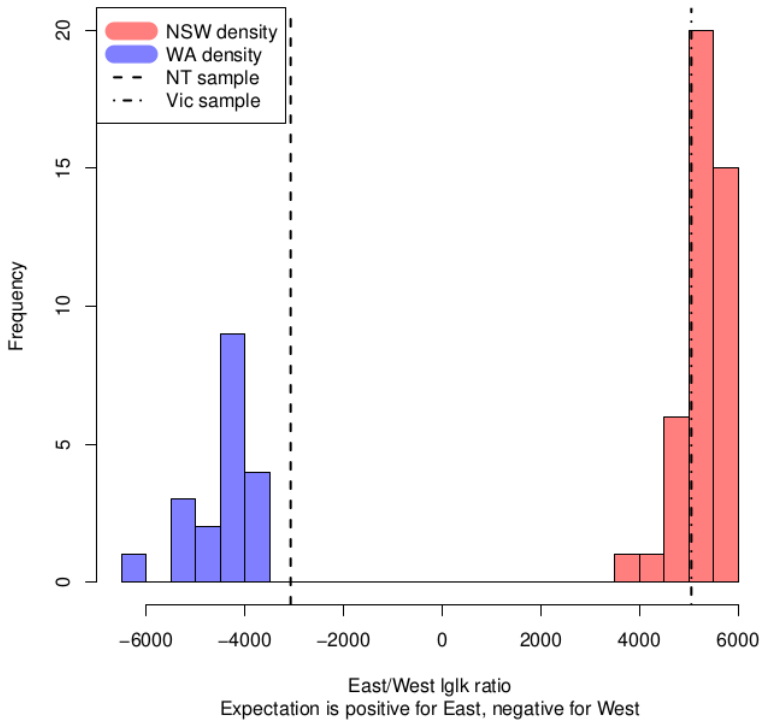

Figure 12. Loglikelihood-ratio test value distributions for New South Wales and Western Australia samples, with dashed lines representing the values for the Northern Territory and Victorian samples.

5.4 Discussion

Based on the likelihood-ratio test, the NT sample is consistent with being a member of the Western population group, with an outside possibility of belonging to another independent population. Because of the impacts of ascertainment bias on the analysis, there is little justification for treating the NT sample as being ‘outlying’ from the Western population, despite the classification statistic value for the NT fish being slightly lower than all known-origin Western samples. To rule out ascertainment bias, future analysis would include large numbers (i.e., several hundreds) of known western and known eastern GNS, which would allow precise population allele frequency estimates to be made for the two potential source populations and leave sufficient samples for an unbiased training-set/testing-set analysis.

6. References

Ahonen H., Stow A. (2009). Population size and structure of grey nurse shark off east and west Australia. Final Report to the Department of Environment, Water, Heritage and the Arts. 18 pp.

Anastasiadi D., Piferrer F. (2020). A clockwork fish: Age prediction using DNA methylation-based biomarkers in the European seabass. *Molecular Ecology Resources*, **20**: 387–397. DOI: 10.1111/1755-0998.13111

Australasiangenomes. (2023). Grey nurse shark (*Carcharias taurus*).

https://awgg-lab.github.io/australasiangenomes/species/Carcharias_taurus.html

Bansemer C. (2009). Population biology, distribution, movement patterns and conservation requirements of the grey nurse shark (*Carcharias taurus*; Rafinesque 1810) along the east coast of Australia. University of Queensland. St Lucia, Queensland, Australia. 143 pp.

Bansemer C. S., Bennett M. B. (2009). Reproductive periodicity, localised movements and behavioural segregation of pregnant *Carcharias taurus* at Wolf Rock, southeast Queensland, Australia. *Marine Ecology Progress Series*, **374**: 215-227. DOI: 10.3354/MEPS07741

Bell C. G., Lowe R., Adams P. D., Baccarelli A. A., Beck S., Bell J. T., Christensen B. C., Gladyshev V. N., Heijmans B. T., Horvath S., Ideker T., Issa J-P. J., Kelsey K. T., Marioni R. E., Reik W., Relton C. L., Schalkwyk L. C., Teschendorff A. E., Wagner W., Zhang K., Rakyan V. K. (2019). DNA methylation aging clocks: challenges and recommendations. *Genome Biology*, **20**: 249 (2019). DOI: 10.1186/s13059-019-1824-y

Branstetter S. and Musick J. A. (1994). Age and Growth Estimates for the Sand Tiger in the Northwestern Atlantic Ocean. *Transactions of the American Fisheries Society*, **123**: 242-254. DOI: 10.1577/1548-8659(1994)123<0242:AAGEFT>2.3.CO;2

Bradford R. W., Thomson R. J., Bravington M., Foote D., Gunasekera R., Bruce B. D., Harasti D., Otway N., Feutry P. (2018). A close-kin mark-recapture estimate of the population size and trend of east coast grey nurse shark. Report to the National Environmental Science Program, Marine Biodiversity Hub. CSIRO Oceans & Atmosphere, Hobart, Tasmania.

https://www.nespmarine.edu.au/document/close-kin-mark-recapture-estimate-population-size-and-trend-east-coast-grey-nurse-shark

Bravington, M. V., Grewe, P., Davies, C. R. (2016a). Close-kin mark-recapture: estimating the abundance of Bluefin tuna from parent-offspring pairs. *Nature Communication*, **7**: 13162. DOI: 10.1038/ncomms13162

Bravington M. V., Skaug H. J., Anderson E. C. (2016b). Close-kin mark-recapture. *Statistical Science*, **31**: 259-275. DOI: 10.1214/16-STS552

Bruce B. D., Bradford R. W., Bravington M., Feutry P., Grewe P., Gunasekera R., Harasti D., Hillary R., Patterson T. (2018). A national assessment of the status of white sharks. National Environmental Science Programme, Marine Biodiversity Hub, CSIRO. https://www.nespmarine.edu.au/document/national-assessment-status-white-sharks

Cardno Ecology Lab (2010). Development and implementation of a population protocol to provide an estimate of the size of the east coast population of grey nurse sharks (*Carcharias taurus*). Department of Environment, Water, Heritage and the Arts, Canberra. 162pp.

Compagno L. J. V. (2001). Sharks of the world. An annotated and illustrated catalogue of shark species known to date. Volume 2. Bullhead, mackerel and carpet sharks (Heterodontiformes, Lamniformes and Orectolobiformes). FAO Species Catalogue for Fishery Purposes. No. 1, Vol. 2. Rome, FAO. 2001. 269pp.

Cropp B. (1964). Shark Hunters. Rigby, Adelaide. Pp. 192. ISBN: 0851793363. Catalogue Persistent Identifier: https://nla.gov.au/nla.cat-vn2284581

Devloo-Delva F. (2021). From rivers to ocean basins – quantifying sex-specific connectivity in sharks. PhD Thesis, University of Tasmania. DOI: 10.25959/100.00046045

Dicken M., Booth A. J., Smale M. J. (2008). Estimates of juvenile and adult ragged tooth shark (*Carcharias taurus*) abundance along the east coast of South Africa. Canadian Journal of Fisheries and Aquatic Sciences, **65**, 621–632

DEWHA (2009). Review of the Grey Nurse Shark Recovery Plan. Department of Environment, Water, Heritage and the Arts, Canberra. 43 pp.

DoE (2014a). Recovery Plan for the Grey Nurse Shark (*Carcharias taurus*). Australian Government Department of the Environment, Canberra. 48 pp.

environment.gov.au/resource/recovery-plan-grey-nurse-shark-carcharias-taurus.

DoE (2014b). Issues Paper for the Grey Nurse Shark (*Carcharias taurus*). Australian Government Department of the Environment, Canberra. 48 pp.

environment.gov.au/resource/recovery-plan-grey-nurse-shark-carcharias-taurus.

Doyle J. J., Doyle J. L. (1987). A rapid DNA isolation procedure for small quantities of fresh leaf tissue. *Phytochemical Bulletin,* **19,** 11-15.

Drew L. (2022). Turning back time with epigenetic clocks. *Nature* **601**, S20-S22 (2022)

DOI: https://doi.org/10.1038/d41586-022-00077-8

Dudgeon C. L., Pollock K. H., Braccini J. M., Semmens J. M., Barnett, A. (2015). Integrating acoustic telemetry into mark–recapture models to improve the precision of apparent survival and abundance estimates. *Oecologia*, **178**, 761-772

Horvath S. (2013). DNA Methylation age of human tissues and cell types. *Genome Biology*, **14**: R115. DOI: 10.1186/gb-2013-14-10-r115

EA (2002). Recovery Plan for the Grey Nurse Shark (*Carcharias taurus*) in Australia. Environment Australia, Canberra. 53 pp. ISBN: 0642547882.

EPBC (1999). *Environmental Protection and Biodiversity Conservation Act*. Department of Climate Change, Energy, the Environment and Water. Canberra, Australia. dcceew.gov.au/environment/epbc

Feutry P., Devloo-Delva F., Tran Lu Y. A., Mona S., Gunasekera R. M., Johnson G., Pillans R. D., Jaccoud D., Kilian A., Morgan D. L., Saunders T., Bax N. J., Kyne P. M. (2020). One panel to rule them all: DArTcap genotyping for population structure, historical demography, and kinship analyses, and its application to a threatened shark. *Molecular Ecology Resour*ces, **20**: 1470–1485. DOI: 10.1111/1755-0998.13204

Feutry P., Kyne P. M., Pillans R. D., Chen X., Naylor G. J. P., Grewe P. M. (2014). Mitogenomics of the Speartooth Shark challenges ten years of control region sequencing. *BMC Evolutionary Biology*, **14**, 232. DOI: 10.1186/s12862-014-0232-x

Friedman J., Hastie T., Tibshirani R. (2010). Regularization Paths for Generalized Linear Models via Coordinate Descent. *Journal of statistical software*, **2010 33(1)**:1-22. Epub 2010/09/03. PubMed PMID: 20808728; PubMed Central PMCID: PMCPMC2929880.

Geweke J., (1992). Evaluating the accuracy of sampling-based approaches to the calculations of posterior moments. *Bayesian Statistics*, **4**, pp.641-649

Gilmore R. G., Dodrill J. W., Linley P. A. (1983). Reproduction and embryonic development of the sand tiger shark, *Odontaspis taurus* (Rafinesque). *Fishery Bulletin* (Wash DC), **81**: 201–225

Goldman K. J., Branstetter S., Musick J. A. (2006). A re-examination of the age and growth of sand tiger sharks, *Carcharias taurus*, in the western North Atlantic: the importance of ageing protocols and the use of multiple back-calculation techniques. *Environmental Biology of Fishes*, **77**: 241-252. DOI: 10.1007/s10641-006-9128-y

IUCN (2023). The IUCN Red List of Threatened Species. Version 2022-2. iucnredlist.org

Conoco Phillips Australia (2017). Barossa Area Development: Offshore Project Proposal

ConocoPhillips document number: BAA-00-EN-RPT-00001 July 2017. Available from: https://www.nopsema.gov.au/sites/default/files/documents/2021-03/Draft-for-public-comment-Barossa-Area-Development-Offshore-Project-Proposal-July-2017.pdf

Kabacik S., Lowe D., Fransen L., Leonard M., Ang S-L., Whiteman C., Corsi S., Cohen H., Felton S., Bali R., Horvath S., Raj K. (2022). The relationship between epigenetic age and the hallmarks of aging in human cells. *Nature Aging*, **2**: 484–493 (2022). DOI: 10.1038/s43587-022-00220-0

King R., Langrock, R. (2016). Semi-Markov Arnason–Schwarz models. *Biometrics*, **72**(2), pp.619-628

Krueger F., Andrews S. R. (2011). Bismark: a flexible aligner and methylation caller for Bisulfite-Seq applications. *Bioinformatics* (Oxford, England), **2011 27(11)**: 1571-2. Epub 2011/04/16. PubMed PMID: 21493656; PubMed Central PMCID: PMCPMC3102221. DOI: 10.1093/bioinformatics/btr167

Laake J. L. (2013). Capture-recapture analysis with hidden Markov models. AFSC Processed Report 2013-04, 34 p. Alaska Fisheries Science Centre, NOAA, National Marine Fisheries Service, 7600 Sand Point Way NE, Seattle WA 98115.

Last P. R., Stevens J. D. (2009). Sharks and Rays of Australia. Second Edition. CSIRO Division of Fisheries, Hobart. 644 pp. ISBN 978-0-674-03411-2.

Lebreton J.D., Nichols J.D., Barker R.J., Pradel R., Spendelow, J.A. (2009). Modeling individual animal histories with multistate capture–recapture models. *Advances in Ecological Research*, **41**, pp.87-173.

Lees K. J., MacNeil M. A., Hedges K. J., Hussey N. E. (2021). Estimating demographic parameters for fisheries management using acoustic telemetry. *Reviews in Fish Biology and Fisheries*, **31**(1), 25-51

Lu J., Johnston A., Berichon P., Ru K-l., Korbie D., Trau M. (2017). PrimerSuite: a high-throughput web-based primer design program for multiplex bisulfite PCR. *Scientific reports*, **2017 7(1)**:1-12.

Lucifora L. O., Menni R. C., Escalante A. H. (2002). Reproductive ecology and abundance of the sand tiger shark, *Carcharias taurus*, from the southwestern Atlantic. *ICES Journal of Marine Science*, **59**: 553–561.

Mayne B., Berry O., Jarman S. (2021). Optimal sample size for calibrating DNA methylation age estimators. *Molecular Ecology Resources,* **21**: 2316–2323. DOI: 10.1111/1755-0998.13437

Mayne B., Korbie D., Kenchington L., Ezzy B., Berry O., Jarman S. (2020). A DNA methylation age predictor for zebrafish. *Aging*, **12**: 24817–24835. DOI: 10.18632/aging.202400

Momigliano P, Jaiteh VF. (2015). First records of the grey nurse shark *Carcharias taurus* (Lamniformes: Odontaspididae) from oceanic coral reefs in the Timor Sea. *Marine Biodiversity Records*. 2015;8:e56. DOI:10.1017/S1755267215000354

Nichols J. D., William L. K. (1995). The use of multi-state capture-recapture models to address questions in evolutionary ecology. *Journal of Applied Statistics*, **22**(5-6): 835-846

Niella Y., Peddemors V. M., Green M., Smoothey A. F., Harcourt R. (2021). A “wicked problem” reconciling human-shark conflict, shark bite mitigation, and threatened species. *Frontiers in Marine Science*, **2**:720741. DOI: 10.3389/fcosc.2021.720741

O’Dea R. E., Noble D. W. A., Johnson S. L., Hesselson D., Nakagawa S. (2016). The role of non-genetic inheritance in evolutionary rescue: Epigenetic buffering, heritable bet hedging and epigenetic traps. *Environmental Epigenetics*, **2**: **dvv014**. DOI: 10.1093/eep/dvv014

Otway N. M., Burke A. L. (2004). Mark-recapture population estimate and movements of grey nurse sharks. New South Wales Fisheries Final Report Series No.63. NSW Fisheries Office of Conservation, Nelson Bay, NSW. 63 pp.

Passerotti M. S., Andrews A. H., Carlson J. K., Wintner S. P., Goldman K. J., Natanson L. J. (2014). Maximum age and missing time in the vertebrae of sand tiger shark (*Carcharias taurus*): validated lifespan from bomb radiocarbon dating in the western North Atlantic and southwestern

Indian Oceans. *Marine and Freshwater Research*, 65, 674–687. http://dx.doi.org/10.1071/MF13214

Patterson T. A., Pillans R. D. (2019). Designing acoustic arrays for estimation of mortality rates in riverine and estuarine systems. *Canadian Journal of Fisheries and Aquatic Sciences*, **76**(9): 1471-1479

Pepperell J. G. (1992). Trends in distribution, species composition and size of sharks caught by gamefish anglers off south-eastern Australia, 1960-90. *Australian Journal of Marine and Freshwater Research*, **43**: 213-225

Petersma F., Thomas L., Harris D., Bradley D., Papastamatiou Y. P. (2024). Age is not just a number: How incorrect ageing impacts close-kin mark-recapture estimates of population size. *Ecology and Evolution* 2024:14:e11352. DOI: 10.1002/ece3.11352

Peterson L. K., Jones M. L., Brenden T. O., Vandergoot C. S., Krueger C. C. (2021). Evaluating methods for estimating mortality from acoustic telemetry data. *Canadian Journal of Fisheries and Aquatic Sciences*, **78** (10): 1444-1454. DOI. 10.1139/cjfas-2020-0417

Piferrer F., Anastasiadi D. (2023). Frontiers in Marine Science, 30 January 2023 Sec. *Marine Fisheries, Aquaculture and Living Resources*, **10 – 2023**. DOI: 10.3389/fmars.2023.1062151

Pollard D. A., Lincoln Smith M. P., Smith A. K. (1996). The biology and conservation status of the grey nurse shark (*Carcharias taurus* Rafinesque 1810) in New South Wales, Australia. *Aquatic Conservation of Marine and Freshwater Ecosystems*, **6**: 1-20. DOI. 10.1002/(SICI)1099-0755(199603)6:1<1::AID-AQC177>3.0.CO;2-#

Reid D. D., Robbins W. D., Peddemors V. M. (2011). Decadal trends in shark catches and effort from the New South Wales, Australia, Shark Meshing Program 1950-2010. *Marine and Freshwater Research*, **62**: 676-693

Stow A., Zenger K., Briscoe D., Gillings M., Peddemors V., Otway N., Harcourt R. (2006). Isolation and genetic diversity of endangered grey nurse shark (*Carcharias taurus*) populations. *Biology Letters*, **2**: 308-311. DOI: 10.1098/rsbl.2006.0441

Tate R. D., Cullis B. R., Smith S. D. A., Kelaher B. P., Brand C. P., Gallen C. R., Mandelman J. W., Butcher P. A. (2019). The acute physiological status of white sharks (*Carcharodon carcharias*) exhibits minimal variation after capture on SMART drumlines. *Conservation Physiology*, **7**(1): coz042. DOI: 10.1093/conphys/coz()

7. Appendix A: CKMR assumptions

The assumption is made that all the rates and probabilities have been stable for several generations, in other words, long enough for the age-structure of the population to have stabilised (i.e. total abundance may be rising or falling exponentially over time, but the relative proportions-at-age are constant from year to year). This is also known as the “quasi-equilibrium” assumption. This assumption covers not only annual proportions-at-age, but any density-dependent effects on reproductive parameters. For example, the quasi-equilibrium assumption would be invalid if the population had started the period in an undepleted state, where per capita reproductive rate is lower than in an already-depleted stock.

The structural assumptions of the CKMR GNS population-dynamics model are:

1. all females mature at a fixed age and all males at a lower fixed age (knife-edge maturity)
2. after maturity, average annual reproductive output is equal for all adults of a given sex
3. annual survival probability is constant over time, sex, and age for ages 7+
4. annual survival probability varies log-linearly with age, between ages 0 and 7
5. average fecundity (female offspring per female adult per year) is fixed over time
6. male-to-female ratio at birth is fixed over time.

In the absence of published data on the age at maturity of eastern Australian GNS, two alternative sets of values were considered (to account for uncertainty in true age-at-maturity) based on the growth curves of Goldman et al. (2006): knife-edged maturity at 10 years old for females and 7 years old for males, or 14 years old for females and 11 years old for males. Fecundity was assumed to be 0.5, based on a presumed average litter size of 1 female and 1 male every other year. All other parameters are estimated from the data using the CKMR model. These parameters include:

- adult abundance (by sex) in some arbitrary reference year
- ratio of adult males to females
- annual rate-of-change of abundance
- adult survival rate per year.

The CKMR probability calculations only estimate the number of adults, and no direct data on juvenile survival is available, thus there is no reliable way to estimate total abundance in the absence of having enough information to estimate juvenile abundance. The question then arises why any assumptions/modelling of juveniles are needed at all for GNS. There are two reasons:

1. Since juvenile survival probabilities cannot exceed 1, the low fecundity of GNS places some constraints on the range of population dynamics, in part on the rate-of-increase/decrease of the population. Therefore, using an explicit model for juvenile survival prevents the model from estimating population growth rates that imply higher birth rates than are biologically possible.

2. Estimates must be made of the ages of the sharks. Those estimates are mainly driven by the probability distribution of length-given-age, which is assumed known from the growth curve (see Appendix A, section A1.3). However, the age-given-length

estimates are also somewhat affected by the underlying distribution of numbers-at-age within the population, which is determined by survival-probabilities-at-age among the juveniles.

In all, the structural assumptions about juvenile survival, fecundity, and age-at-maturity should not— even if slightly wrong— have much effect on the estimates of adult dynamics obtained in this project as juvenile survival was estimated given the chosen values for fecundity and age-at-maturity. The model is able to vary its estimate of juvenile survival in order to give the best fit to the information that the close-kin data provide regarding the adult population. The main question is whether the quasi-equilibrium assumption is appropriate for modelling all our samples. If reasonably accurate age estimates were available for the GNS sample, this problem could be avoided by omitting kinship comparisons on pairs where the relevant dates-of-birth are far back in time. However, because most of the length measurements are inaccurate, the possibility that those individuals were born a long time ago cannot be excluded, thus the more complicated model and more ambitious assumptions are inevitable.

At face value, the structural assumptions seem either uncontroversial given GNS biology, or unlikely to have much impact on the final answer even if the details are wrong. For example, some assumption has to be made about juvenile survival rates, similar but not necessarily identical to #4 above (annual survival probability varies log-linearly with ages 0-7 years), in order to make the model internally coherent. But the details of that particular assumption should only have a small impact on the abundance estimates, compared to sampling noise, including uncertainties in the dataset. Furthermore, whether maturity happens to all female GNS at exactly the same age (knife-edge), or whether it is spread out over a few years, should have little effect on the final answer.

8. Appendix B: Population dynamics equations and CKMR probabilities

Reproduced from Bradford et al. (2018).

Table 7. Notation used in the equations describing the Close-Kin Mark-Recapture model. Note that subscripts (e.g. regarding age, sex, and sample) have been suppressed for clarity.

Symbol	Meaning
$\mathrm{I}[], \mathbb{P}[]$	indicator function (1/0) and probability of some event
i, j	"labels" denoting particular animals being considered
x	whether the animal was sampled DEAD or ALIVE
s	sex
y, y_{ref}	year (of sampling, or generally); y_{ref} is an arbitrary "reference year" for abundance
a	age
b	year of birth, i.e. $y - a$
α	age at maturity
$\mathtt{a}$	age when survival probability reaches its adult value. $\mathtt{a} \leq \min(\alpha_{♀}, \alpha_{♂})$
N_a; N^{ad}	number of juveniles aged a; number of adults
p_a; p^{ad}	annual survival probability of juveniles aged a; and of adults

r	annual rate-of-increase/decrease of the population (1→constant)
b	fecundity (age-0 offspring per female per year). Also determines sex ratio.
β	slope of stable-age-composition in adults
π	stable-age-composition probabilities in juveniles
v	"nuisance parameters" required for handling same-cohort comparisons

The population-dynamics model is entirely age-based, with knife-edge maturity. In terms of the notation above (Table 1), we have:

$$N_{s,y+1}^{ad} = p^{ad} N_{s,y}^{ad} + p_{\alpha-1} N_{s,\alpha-1,y}$$

$$N_{s,a+1,y+1} = p_a \, N_{s,a,y} \qquad 0 < a < \alpha$$

$$N_{s,0,y+1} = b_s \, N_{\varphi,y}^{ad} \qquad 0 < a < \alpha$$

$$\log(p_a) = \frac{a}{\mathrm{a}} \log\left(p^{ad}\right) + \frac{(a-\mathrm{a})}{\mathrm{a}} \log(p_0)$$

In addition, the assumption of quasi-equilibrium leads to an implied solution for the rate-of-change, *r,* and the population age-composition of juveniles and adults (given by π and $\boldsymbol{\theta}$) in terms of the other parameters, as the eigensolution of the Leslie matrix (see Hillary *et al*. 2018b for details). The setup for GNS is simple enough in that that there are in fact closed-form expressions for r, π, or $\boldsymbol{\theta}$, but the formulae are omitted here for brevity. In the notation of this paper, we have:

$$N_{s,y+1}^{ad} = r \, N_{s,y}^{ad} = r^{y-y\mathrm{ref}} \, N_{s,y\mathrm{ref}}^{ad}$$

$$N_{s,a+1,y} = \beta \, N_{s,y,a}; \qquad a \geq \mathrm{a}$$

$$N_{s,a,y} = \alpha \, \pi_a \, ; \qquad a \geq \alpha$$

Note that the stable-age-composition of juveniles, $\{\pi_a;\ \ a < \alpha\}$, is not a geometric progression because survival probability varies with age; it is used only in computing posterior probabilities of age given measured length.

All of the CKMR probabilities follow the expected relative reproductive output (ERRO) principles given in Bravington *et al*. (2016a), specialised to the circumstances assumed for GNS. The equations below are expressed purely in terms of age, which is assumed to be the fundamental biological variable; in practice we only have length estimates for GNS, so the equations need to be adapted as described in section A1.3.

For POPs we have:

$$\mathbb{P}\left[Kij = \mathrm{PO} \middle| s_i, x_i, y_i, a_i, b_j, \right] = \mathrm{I}\left[a_i - \left(b_j - y_i\right) \geq \alpha_{s_i}\right] * \frac{1}{N^{ad}_{s_i, b_j}} * \begin{cases} \mathrm{I}\left[y_i \geq b_j\right] & x_i = \mathrm{ALIVE} \\ \prod_{a=a_i}^{a_i + \max(0, b_j - y_i) - 1} (p_a) & x_i = \mathrm{DEAD} \end{cases}$$

The three terms represent, respectively:

i must be mature when *j* is born

all the adults of *i*'s sex that are alive when *j* is born have an equal chance of being the relevant parent

i still has to be alive at *j*'s birth.

For HSPs where the shared-parent's sex is s, we have:

$$\mathbb{P}\left[Kij = s - \mathrm{HSP} | b_i, b_j; b_j > b_i\right] = \frac{1}{N^{ad}_{s_i, b_j}} * p^{ad(b_j - b_i)}$$

where "s-HSP" indicates that the possible kin types are maternal-HSP or paternal-HSP. The point here is that the parent was clearly alive and mature when *i* was born. To have a chance of being *j*'s parent it needs to survive the intervening period until *j*'s birth (the rightmost term) and then has an equal chance of parenthood as any other living adult of that sex at that time. When $b_i = b_j$ (i.e. same-cohort HSPs) this needs to be multiplied by an additional parameter v_s, as explained in section A4.3.

For GGPs where the sex of the "intervening" parent is s, we have to consider all possible ages, a^*, of the unobserved intervening parent, given that (s)he was evidently mature at *j*'s birth. Given some possible age, a^*, the question is whether his/her parent was actually animal *i*— which requires *i* to be alive and mature at the birth of the intervening parent, i.e. at $b_j - a^*$. Conceptually, this entails summing the POP probability over an infinite range of possible intervening-parent birth-years. The result is:

$$\mathbb{P}\left[Kij = s - \mathrm{GPGC} \middle| s_i, x_i, y_i, a_i, b_j\right] = \sum_{a^* \geq \alpha_s} \mathbb{P}[a^* | a^* \geq \alpha_s] * \mathrm{I}\left[a_i - \left(b_j - a^* - y_i\right) \frac{1}{N^{ad}_{s_i, b_j - a^*}}\right] * \begin{cases} \mathrm{I}\left[y_i \geq b_j - a^*\right] & x_i = \mathrm{ALIVE} \\ \prod_{a=a_i}^{a_i + \max(0, b_j - a^* - y_i) - 1} (p_a) & x_i = \mathrm{DEAD} \end{cases}$$

Note that, although GGPs and HSPs cannot be individually distinguished just using DNA, there is a *statistical* difference in the probability of sharing mtDNA. A GGP will have identical by descent (*ibd)* mtDNA if-and-only-if the elder is female *and* the intervening parent is also female. For HSPs, *ibd* only requires that the shared-parent be a mother, so the sex of the two kin is irrelevant. Of course, mtDNA can be shared even if not *ibd*, so this is not individually definitive, but it does help in the context of a CKMR model. In other words, there is useful information in how the proportion of shared mtDNA in HSPs/GGPs varies with the likely birth-gap between the members of the pair. The problem with GGPs, though, is that to compute the probability, we need to assume that the population-dynamics-assumptions have applied for a very long time.

9. Appendix C: CKMR model output

Table 8. Estimated quantities of interest, N_xxxx: adult population size in year xxxx, M:F: adult male to female ratio, r: population growth rate, p_^ad: adult survival rate, -lnL: negative log likelihood, expected numbers of POPs, HSPs and GGPs and the proportion of HSP/GGPs that share the same mitochondrial DNA haplotype. Observed values are shown in italics in the header. Model scenarios are described in the text. Assumed age-at-maturity is denoted by a_{mat}. The most plausible model is highlighted.

Model	Data	a_{mat}	VB	N_{1975}	N_{2017}	N_{2023}	M:F	*R*	p^{ad}	-lnL	#POPs	#HSPs	#GGP	% mt same
High a_{mat}	Old	14,11	USA	262 (0.50)	1,686 (0.22)	-	1.1	4.5%	0.95	1,113	43*	73*	18*	49%
Low a_{mat}	Old	10,7	USA	489 (0.72)	2,167 (0.21)	-	1.3	3.4%	0.97	1,119	48*	58*	28*	48%
Rev len	Old	10,7	USA	178 (0.34)	2,219 (0.24)	-	1.3	6.2%	0.93	1,117	48*	60*	26*	48%
[1]New	New	10,7	USA	87 (0.34)	1,603 (0.19)	2,431 (0.25)	1.8	7%	0.94	1,282	37†	89†	40†	56%
[2]New laa	New	10,7	Aus[1]	129 (0.54)	1,054 (0.15)	1,423 (0.18)	1.4	5%	0.95	1,277	25	115	27	54%
[3]Slow K	New	10,7	Aus[4]	100 (0.34)	2,317 (0.26)	3,628 (0.33)	1.6	8%	0.95	1,292	44	83	40	54%

The model uses a single growth curve calculated from combined male and female samples with: [1]: t_0 estimated; [2]: fixed at -2.5 years; [3]: slower growth on length-at-age.

CONTACT

Russell Bradford

russ.bradford@csiro.au

This project is supported with funding
from the Australian Government under the
National Environmental Science Program.